

Minimal Thermodynamic Cost of Computing with Circuits

Abhishek Yadav^{1,2,†}, Mahran Yousef^{3,†,*}, and David Wolpert^{1,4,5,6}

¹*Santa Fe Institute, 1399 Hyde Park Road Santa Fe, NM 87501, USA*

²*Department of Physical Sciences, IISER Kolkata, Mohanpur 741246, India*

³*Independent Researcher*

⁴*Complexity Science Hub, Vienna, Austria*

⁵*Arizona State University, Tempe, AZ 85281, USA*

⁶*International Center for Theoretical Physics, Trieste 34151, Italy and*

[†]*Equal Contributions*

All digital devices have components that implement Boolean functions, mapping that component's input to its output. However, any fixed Boolean function can be implemented by an infinite number of circuits, all of which vary in their resource costs. This has given rise to the field of circuit complexity theory, which studies the minimal resource cost to implement a given Boolean function with any circuit. Traditionally, circuit complexity theory has focused on the resource costs of a circuit's size (its number of gates) and depth (the longest path length from the circuit's input to its output). In this paper, we extend circuit complexity theory by investigating the minimal thermodynamic cost of a circuit's operation. We do this by using the mismatch cost (MMC) of a given circuit that is run multiple times in a row to calculate a lower bound on the entropy production (EP) incurred in each such run. Specifically, we discuss conditions under which MMC of a circuit is proportional to the size of a circuit, and when they are not. We also use our results to compare the thermodynamic costs of different circuit families implementing the same family of Boolean functions. In addition, we analyze how differences in the underlying physics of individual gates within a circuit influence the minimal thermodynamic cost of the circuit as a whole. These results lay the foundation for extending circuit complexity theory to include mismatch cost as a resource cost.

I. INTRODUCTION

Computational complexity theory explores the relative difficulty of computing functions within formal models of computation. In his foundational work [1], Alan Turing introduced the concept of Turing machines and demonstrated that functions can be classified as either computable or non-computable. Within the class of computable functions, it was later shown that some are inherently harder to compute than others [2, 3]. Computational complexity theory [4] studies a fundamental question: what does it mean for one function to be more difficult to compute than another?

A given function can often be computed using multiple algorithms, each incurring different resource costs depending on the model of computation. Traditionally, computational complexity theory has focused on quantifying resource usage such as the number of computational steps or memory requirements. Early discussions on complexity measures also considered physical energy expenditure and thermodynamic work as potential complexity metrics [5].

Landauer and Bennett were among the first to explore the thermodynamic cost of computation using equilibrium statistical mechanics. They famously argued that erasing a single bit of information necessarily generates at least $k_B \log 2$ of heat, where k_B is Boltzmann's constant and T is the temperature of the surrounding heat bath [6, 7]. However, this early work modeled computation—which is inherently a non-equilibrium

process—within the framework of equilibrium thermodynamics. As a result, the analysis was semi-formal and limited in scope, leaving many fundamental questions unanswered. At the time, the theoretical tools needed to rigorously analyze far-from-equilibrium systems were not yet available, and the thermodynamics of computation remained an open and underdeveloped area.

Fortunately, recent advances in non-equilibrium thermodynamics, particularly within the framework of stochastic thermodynamics, have made it possible to rigorously define and analyze thermodynamic quantities such as work, entropy, and heat dissipation in systems driven far from equilibrium [8, 9]. These tools are now being applied to fundamental questions about the thermodynamic costs of computation and communication processes [8–12]. In particular, stochastic thermodynamics allows us to analyze the entropy production, i.e., the dissipated heat, in a process.

Boolean circuits provide an alternative model of computation, characterizing the complexity of a function in terms of the size and depth of the circuit implementing it. The size of a circuit is the total number of gates, while the depth corresponds to the longest path from an input to an output, representing the time required for computation [4, 13]. Just as there exist multiple algorithms for a given problem, there are infinitely many Boolean circuits that can implement a given Boolean function. The task of identifying the most efficient circuit among those infinitely many circuits is both theoretically difficult and practically important. Circuit complexity theory pro-

vides a framework for comparing and optimizing circuits based on size (number of gates) and depth (longest path from input to output), but the associated thermodynamic cost of running a circuit as a key measure in optimization has not been given considerable attention.

In this paper, we introduce the use of resource costs grounded in stochastic thermodynamics, in contrast to the traditional resource costs such as size and depth that have been analyzed for algorithms run on a Boolean circuit. Specifically, we focus on the use of mismatch cost (MMC) [11, 14–17]. MMC is defined as the portion of total entropy production that arises when the actual distribution of inputs differs from the distribution a machine is optimized for, and it is largely independent of the microscopic physical details of the implementation. In this sense, MMC strengthens the second law by providing positive lower bounds on the energetic cost of running a computational machine. In the context of circuits, this implies positive lower bounds on the entropy production of running a Boolean circuit that hold regardless of the detailed physics of the gates, depending only on the circuit topology and the way computation proceeds through the gates, as we show in this paper.

For theoretical computer scientists, this work opens up a natural extension of circuit complexity by adding an energetic dimension based on MMC, thereby refining how one compares architectures that implement the same input–output map—not only by depth and size, but also by their associated MMC. Additionally, the scaling behavior of MMC with respect to problem size — analogous to other resource costs — opens up a particularly interesting direction. Moreover, other resource costs such as “time” and “space” that are of deep interest in CS theory are only defined for specific computational architectures, e.g., Turing Machines, Boolean circuits, or DFAs. While the definitions for these costs are analogous to one another, and in some cases are related up to polynomial transformations, they are formally different. In contrast, MMC is an architecture-independent resource cost: the *exact same* definition applies across computational architectures. Additionally, unlike purely abstract notions of computational complexity, MMC is partially informed by properties of the physical system implementing the computation, and can therefore be interpreted as a very coarse proxy for real-world energetic costs.

Circuit design provides an important example of the power of using MMC as the resource cost. A central challenge in digital circuit design is how to trade off different resource costs when implementing a desired computation [18, 19]. Energetic costs, and the associated heat dissipation, are a major concern. As processors grow smaller and more efficient [20] approaching thermodynamic limits, and as computational demands continue to grow—particularly due to large-scale data processing and machine learning workloads—understanding the energy cost of computation is becoming increasingly impor-

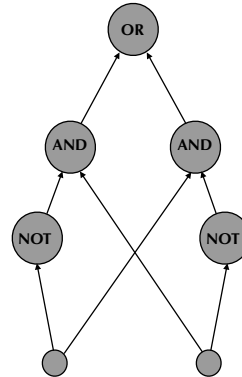


FIG. 1. An example of a 2-input and 1-output circuit with a topological ordering.

tant [21]. Much prior circuit-level energy analysis relies on phenomenological power models and electrical dissipation estimates (e.g., CMOS power models and Joule heating in interconnects), rather than on thermodynamically grounded lower bounds [19, 22, 23].

In contrast, incorporating non-equilibrium thermodynamic considerations into circuit complexity theory provides a principled framework for quantifying minimal heat dissipation in circuits. This perspective can refine existing complexity measures and help inform the design of architectures that are both logically and thermodynamically efficient. Moreover, since circuit structure determines whether a function is efficiently parallelizable or inherently sequential [24], thermodynamic analysis can shed light on the energy efficiency of parallel computation. Taken together, the framework we introduce provides a bridge between questions traditionally studied in statistical physics, computer science, and information theory, by placing them under a common energetic notion of computational cost.

A. Contributions and roadmap

This paper presents several key contributions aimed at understanding the thermodynamic cost of computation in Boolean circuits. First, we derive a lower bound on the EP arising in running Boolean circuits. This bound emerges primarily from the modular structure of circuits, where the dynamics of gates depend on the states of only a subset of gates, creating a network of dependencies that govern the flow of logic and dynamics. Based on this bound, we introduce a new circuit complexity measure—mismatch cost complexity. We also establish formal relationships between MMC complexity and traditional size

complexity. Additionally, we compute the MMC complexity for various circuit families that implement the same Boolean function, enabling a comparison of their thermodynamic efficiency.

The structure of the paper is as follows: In Sec. II A, we provide a minimal background on circuit complexity theory, reviewing the concepts of circuit families, size and depth complexity, and their associated complexity classes. In Sec. II B, we briefly review stochastic thermodynamics and the MMC lower bound on EP. In Sec. III, we focus on determining MMC of a circuit. The circuit diagram alone does not specify the dynamical changes of the circuit's state, i.e., of the joint distribution over the circuit's gates as it runs. In Sec. III A we explain what other information is needed, and how to use it to calculate that change in the state of a circuit evolves during its execution. In Sec. III B and Sec. III C we combine these results, to derive the expression for the total MMC in computation with circuits.

Sec. IV builds on this analysis to introduce *mismatch cost complexity* as a new circuit complexity measure, analogous to size and depth complexity, representing the minimal energetic cost of implementing a Boolean function with any circuit. We derive results and theorems that link MMC complexity to size complexity, showing that under certain conditions, the upper bound on MMC grows linearly with the size complexity of a circuit family. Complementing this result, we identify conditions where MMC scales differently from size complexity. In Sec. V, we discuss the energetic aspects of circuit optimization by comparing the MMC associated with circuit families that implement a given Boolean function. Specifically, we study two families that compute the ADD function—one with depth complexity $\log(n)$ and another with n . We also investigate the impact of heterogeneity in the physical properties of gates on the associated MMC. Finally, Sec. VI concludes the paper by discussing possible directions for future research.

B. Earlier work

The tools of stochastic thermodynamics have been applied to computational models such as finite automata [11, 16, 25] and Turing machines [26, 27], providing one of the first principled frameworks for analyzing the thermodynamic costs of computation. Specific to circuits, prior work has estimated the heat dissipated during gate operations using Landauer's bound [28]. While this was a pioneering approach, stochastic thermodynamics now recognizes that the Landauer bound—which accounts only for entropy changes—can be zero even when the total dissipated heat is substantial [29]. This highlights the importance of entropy production (EP), a central concept in stochastic thermodynamics.

More recent studies have incorporated EP into the

analysis of Boolean circuits by modeling gate dynamics as continuous-time Markov chains (CTMCs) [30]. However, such a framework requires properly incorporating dynamics over hidden states, which in general are necessary for there to be a CTMC that can implement discrete-time dynamics [31]. In contrast, our analysis does not assume any specific form for the underlying continuous-time dynamics. Furthermore, in our model, the logical values at gates are not reset between successive runs, more closely reflecting the behavior of many physical computing devices. In contrast, prior work [30] assumes a full reset after each computation.

Another closely related set of results analyzes entropy production in stochastic processes structured as Bayesian networks [32–34]. These works provide general decompositions of entropy production in terms of information flows along the edges of a directed acyclic graph. The formalism developed in those works is in principle extensible to circuit-like architectures, and our framework can be viewed as a specialization of these more general thermodynamic decompositions to Boolean circuits, together with a complexity-theoretic perspective on how costs scale with circuit size.

II. BACKGROUND

A. Circuit complexity theory

In this section, we provide a brief and necessarily compact overview of basic concepts from circuit complexity theory. For a more detailed and comprehensive treatment, see [4].

A circuit is built from basic logic gates that are interconnected to process inputs and produce outputs (Fig. 1). A *basis* is a set \mathcal{B} of Boolean functions that define the allowable gates in a circuit. For example, a basis containing AND and NOT gates is considered a *universal basis* because any Boolean function can be implemented using only these gates. Formally, a Boolean circuit is represented as a *directed acyclic graph* (DAG), denoted by $(V, E, \mathcal{B}, \mathcal{X})$, where V is the set of nodes representing a logic gate selected from a finite basis \mathcal{B} . The set of edges E define the directed connections between gates, determining how information flows through the circuit. The set \mathcal{X} represents the state space of the circuit (see below). The direction of edges reflects dependencies between gates, enabling a specific ordering of nodes in V . This ordering, called a *topological ordering*, ensures that for every directed edge from node μ to node ν , node μ appears before node ν in the sequence ($\mu < \nu$).

A node μ has incoming edges from nodes known as its *parent nodes*, denoted as $\text{pa}(\mu)$, and outgoing edges to nodes known as its *children nodes*, denoted as $\text{ch}(\mu)$. Nodes that have no incoming edges, called *input nodes* or *root nodes*, serve as the circuit's inputs. We denote the

set of input nodes as $V_{\text{in}} \subset V$ and the set of all non-input nodes as $V_{\text{nin}} = V \setminus V_{\text{in}}$. Each gate μ in the circuit has an associated state space, denoted by X_μ , and its state is represented by $\mathbf{x}_\mu \in X_\mu$. For binary gates, the state space is $X_\mu = \{0, 1\}$. The collective states of all gates together define the *joint state* of the circuit. The *joint state space* of the circuit is given by

$$\mathcal{X} = \bigotimes_{\mu} X_\mu$$

and the *joint state* of the circuit is denoted by \mathbf{x} .

We use $\mathbf{x}_{\text{pa}(\mu)}$ and $\mathbf{x}_{\text{ch}(\mu)}$ to denote the joint state of the parent and children gates of a gate μ , respectively. Similarly, we define \mathbf{x}_{in} and \mathbf{x}_{nin} to represent the joint states of all input nodes and all non-input nodes, respectively.

The *size* of the circuit is defined as the total number of gates, or $|V|$. The *depth* of the circuit is defined as the length of the longest path from an input node to an output node. Circuit size and depth are two important complexity measures of a circuit, they also provide a measure of the hardness of computation of a function f as the size and depth of the minimal circuit that computes it.

An n -input Boolean function is a mapping

$$f^n : \{0, 1\}^n \rightarrow \{0, 1\}^m,$$

which takes n -bit binary inputs and produces m -bit binary outputs. A *family of Boolean functions* is defined as a sequence $f = \{f^n\}_{n \in \mathbb{N}}$, where each f^n corresponds to a specific input size n . This formulation allows us to define an associated function

$$f : \{0, 1\}^* \rightarrow \{0, 1\}^*,$$

that operates on inputs of arbitrary length. For example, consider the addition function

$$\text{ADD}^n : \{0, 1\}^{2n} \rightarrow \{0, 1\}^{n+1}$$

which takes two n -bit binary representations of natural numbers and outputs their sum in binary. The function family $\{\text{ADD}^n\}_{n \in \mathbb{N}}$ extends this addition operation to all possible input sizes.

Circuits differ fundamentally from other models of computation. In models like Turing machines, a single machine accepts input of any arbitrary length. In contrast, circuits require a distinct specification for each input length. This means that to compute functions belonging to the same family but with different input sizes, one must design distinct circuits for each case. Because the model does not provide a uniform mechanism for handling all input lengths, it is classified as a *non-uniform* model of computation [4, 13]. As a result, computation in this model is described using a *circuit family*, denoted as $\{C_n\}_{n \in \mathbb{N}}$, where each circuit C_n corresponds to inputs

of length n . A circuit family \mathcal{C} is a sequence $\{C_n\}_{n \in \mathbb{N}}$ of Boolean circuits, where C_n is the circuit with n inputs. A circuit family \mathcal{C} is said to compute a function f if, for every input string w of length n , the circuit correctly evaluates the function:

$$f^n(w) = C_n(w)$$

for all $n \in \mathbb{N}$. The *size complexity* of a circuit family is the number of gates in n as a function of n , while the *depth complexity* is the length of the longest directed path from an input node to an output node, also expressed as a function of n .

Definition 1 (Size and depth complexity) *A circuit family of size complexity $s(n)$, for a function $s : \mathbb{N} \rightarrow \mathbb{N}$, is any circuit family where the size $|C_n| \leq s(n)$ for every n .*

Analogously, a circuit family of depth complexity $d(n)$, for a function $d : \mathbb{N} \rightarrow \mathbb{N}$, is any circuit family where the depth of $C_n \leq d(n)$ for every n .

Likewise, one can define the size and depth complexity of a function f as the size and depth complexity of the associated circuit family that computes it.

Definition 2 (Circuit complexity class) *Let*

$s : \mathbb{N} \rightarrow \mathbb{N}$. **SIZE**(s) *is the class of functions f for which there exist a circuit family \mathcal{C} of size complexity s .*

*Analogously, let $d : \mathbb{N} \rightarrow \mathbb{N}$. **DEPTH**(d) is the class of functions f for which there exist a circuit family \mathcal{C} of depth complexity d .*

The growth of a circuit's size or depth with respect to the input length of a function provides a crucial measure of the function's computational complexity. In his seminal work, Shannon proved that most Boolean functions require circuits of exponential size, specifically showing that there exist functions that cannot be computed by circuits smaller than $2^n/10n$. In other words, the vast majority of functions—often referred to as "hard" functions—such that $f \notin \text{SIZE}(2^n/10n)$ and thus require exponentially large circuits to compute [35]. However, despite this result, explicitly identifying such a function has remained challenging, as most functions of practical interest can still be computed by circuits of reasonable, albeit large, size.

An interesting class of functions emerges when restricted to "small" circuits, i.e., circuit families whose size does not grow faster than polynomial with input length. \mathbf{P}/poly is the class of functions for which there exist a $\text{poly}(n)$ -size circuit family,

$$\mathbf{P}/\text{poly} := \cup_{c \geq 0} \text{SIZE}(n^c).$$

The class \mathbf{NC}^d consists of functions that can be computed by a circuit family of polynomial size $\text{poly}(n)$ and

depth at most $\log^d n$, for some $d \in \mathbb{N}$. Since the depth, which represents the maximum number of computation steps, grows at most as a logarithmic function of the input size raised to the power of d , the functions in \mathbf{NC}^d can be computed very quickly. These classes form the \mathbf{NC} hierarchy, which is defined to capture the notion of problems that have very fast parallel algorithms using a feasible amount of hardware.

$$\mathbf{NC} = \bigcup_d \mathbf{NC}^d.$$

A function has an efficiently parallel algorithm if and only if it is in \mathbf{NC} [4, 13].

The previous example of ADD is in \mathbf{NC} . However, just like any Boolean function, ADD has many circuit families that can implement it. For example, ADD can be implemented using two well-known circuit families: the ripple-carry adder (RCA) and the carry look-ahead adder (CLA), each offering distinct trade-offs in size and depth complexity [13].

The RCA follows the simple "carry-over" method taught in high school arithmetic, where each bit addition depends on the carry from the previous bit. As a result, for an n -bit input, the depth of the circuit grows linearly with n . Additionally, increasing the input size by one bit requires adding one additional full-adder circuit to the chain. This means that the overall circuit size also grows linearly with n . Its simplicity makes it easy to scale. However, since each stage of bit addition must wait for the carry from the previous stage before proceeding, RCA becomes significantly slower as the input size increases.

In contrast, CLA uses a more sophisticated approach by predicting carry bits in advance rather than waiting for them to propagate sequentially. This significantly reduces the depth of the circuit, which grows proportionally to the logarithm of the input size. As a result, computation time decreases drastically compared to RCA. However, the parallel computation and complex wiring cause the total number of gates in the circuit to grow at a rate proportional to $\log n$. Consequently, as the input size increases, the CLA circuit becomes increasingly intricate.

This exemplifies the trade-offs involved in designing a circuit family to implement a Boolean function. In addition to size and depth, another crucial complexity measure is the energy dissipated in a circuit, which has not yet been considered. In the next section, we briefly introduce stochastic thermodynamics and its framework for computing irreversible heat dissipation in a circuit. This provides an additional complexity measure, analogous to size and depth, that quantifies the energetic cost of a circuit family.

B. Stochastic Thermodynamics and Mismatch Cost

Real-world computational systems operate far from equilibrium, with multiple interdependent components evolving rapidly. Traditional equilibrium statistical mechanics, which applies only to large macroscopic systems that either evolve quasi-statically or remain static, is inadequate for analyzing the energetic costs of computation [12]. Mesoscopic systems far from equilibrium that exhibit stochastic fluctuations can be analyzed within the framework of stochastic thermodynamics. The key assumption in this framework is that any degrees of freedom not explicitly described by the system's dynamics—such as internal states or the reservoirs—remain in equilibrium. This assumption allows one to relate thermodynamic quantities to system dynamics through the principle of local detailed balance [9, 36–38].

One of the central quantities in stochastic thermodynamics is entropy production, which quantifies the irreversible heat dissipation in a process. If the probability distribution over the states of a physical system during its evolution changes from p_0 to p_τ , the total EP associated with an initial distribution p_0 can be expressed as [8, 15],

$$\sigma(p_0) = Q(p_0) - [S(p_\tau) - S(p_0)], \quad (1)$$

where $Q(p_0)$ is called the *total entropy flow* and it corresponds to the change in the thermodynamic entropy of the environments during the process. If the system interacts with N heat reservoirs, the total entropy flow is given by the sum of the energy exchanged with each reservoir, weighted by the inverse of its temperature:

$$Q = \sum_{i=1}^N \frac{Q_i}{T_i}, \quad (2)$$

where Q_i represents the net energy flow into i -th reservoir at temperature T_i , and k_B is Boltzmann's constant. In the context of computation, let X represents the logical states of a computer and G describes a computational map such that after the end of computation, an initial distribution p_0 evolves to $p_\tau(x') = \sum_x G(x'|x)p_0(x)$, or as a shorthand $p_\tau = Gp_0$.

Another important contribution to the EP of running a system is its "mismatch cost". Consider the initial distribution q_0 that minimizes the EP generated by running a system, given in Eq. (1). In the literature, this distribution is referred as the "prior" distribution of the running the system. The reason for this terminology is that q_0 plays the role of a Bayesian prior for an agent trying to change the distribution that the system has at the end of running the system back to the original distribution that the system had *before* the system ran — all while expending the minimal amount of free energy. In particular, that agent must perform a Bayesian inverse to

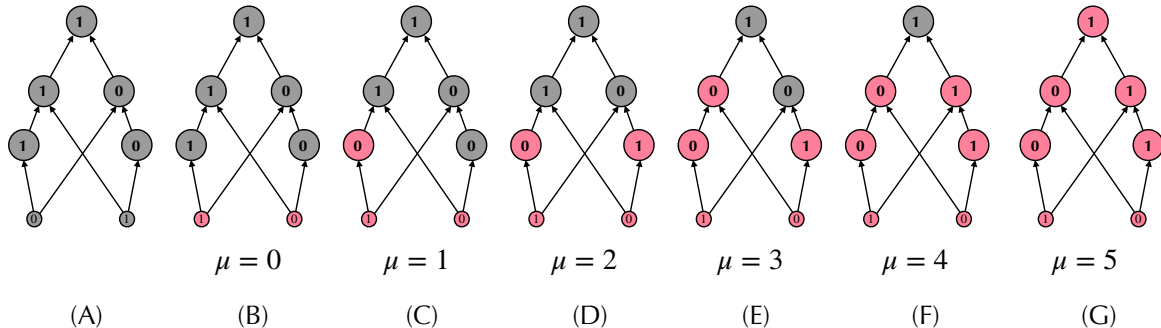


FIG. 2. State space dynamics of a circuit computation. (A) The circuit begins in a state inherited from the previous run, with all gate values logically dependent according to the circuit structure. (B) The inputs are updated for the new run, resetting their values independently of the rest of the circuit. (C–G) Gates are sequentially updated based on their input dependencies, progressively building logical correlations as computation unfolds.

estimate what that original distribution over the states of that system were before that system ran, and q is the proper choice for the prior of this Bayesian inverse [39].

When the process starts from a different initial distribution p_0 , the resulting EP, $\sigma(p_0)$, can be decomposed as [14, 15],

$$\sigma(p_0) = [D(p_0||q_0) - D(Gp_0||Gq_0)] + \sigma_{\text{res}}, \quad (3)$$

where $D(p_0||q_0)$ is the Kullback-Leibler (KL) divergence between p_0 and q_0 , and σ_{res} , known as the residual EP, represents the minimum EP of the process, defined as $\sigma_{\text{res}} := \sigma(q_0)$. The drop in KL-divergence $D(p_0||q_0) - D(Gp_0||Gq_0)$ is called the mismatch cost. The MMC is always non-negative, a consequence of the data processing inequality for KL-divergence. Unlike the residual EP σ_{res} , which depends on the fine details of the physical implementation, MMC depends only on the computational map G , the initial distribution p_0 , and the prior distribution q_0 . All of the physical details of the system are encoded in the choice of the prior. Additionally, σ_{res} is non-negative due to the second law. In certain dynamical situations, the MMC provides a strictly positive contribution to EP.

Consider a process where the computational map G is repeatedly applied to the state space. Since the underlying physical process implementing G remains unchanged across iterations, the prior distribution q_0 also remains the same. However, the actual state distribution evolves with each iteration: after the i -th iteration, it is given by $p_i = Gp_{i-1}$, or more generally, $p_i = G^i p_0$. The total MMC then accumulates over iterations as:

$$\mathcal{MC}(p_0) = \sum_{i=0}^{\tau} D(G^i p_0||q_0) - D(G^{i+1} p_0||Gq_0) \quad (4)$$

Even if the process starts at the prior q_0 , after the first iteration, the distribution becomes $p_1 = Gq_0$, which dif-

fers from q_0 . This deviation from the prior distribution results in a strictly positive MMC in the next iteration, and the same holds for subsequent iterations [11].

Importantly, this strictly positive lower bound on EP holds for any initial distribution p_0 , regardless of the prior q_0 . As the system evolves through a sequence of distributions $\{p_0, p_1, \dots, p_\tau\}$, where $p_{t+1} = Gp_t$, there exists a distribution \hat{q}_0 that minimizes the expression on the right-hand side of Eq. (4). The associated MMC, denoted as $\mathcal{MC}_{\hat{q}_0}(p_0)$, provides a strictly positive lower bound on the actual MMC, regardless of the prior distribution q_0 .

Thus, this strictly positive periodic MMC contribution to EP is entirely independent of the underlying physical process and is fundamentally tied to the computational map G and its repeated application, which highlights the unavoidable EP contribution intrinsic to the computation. In the next section, we describe how the probability distribution over a circuit's states evolves during execution, and how the mismatch between the evolving distribution and the optimal prior distribution contributes to the EP.

III. MISMATCH COST OF COMPUTING WITH CIRCUITS

A. Dynamics of the circuit

A circuit diagram alone does not specify the dynamics of the joint state of the physical circuit, the order in which the gates are run, and how the state of each gate updates, etc. In this section, we introduce one relatively simple way to specify these details from the circuit diagram.

In this specification, the gates are run serially, one after the other. The topological ordering of a circuit determines the sequence in which its gates are executed. Accordingly, we use the topological index μ as a step index, meaning that gate μ updates its value at step μ (see

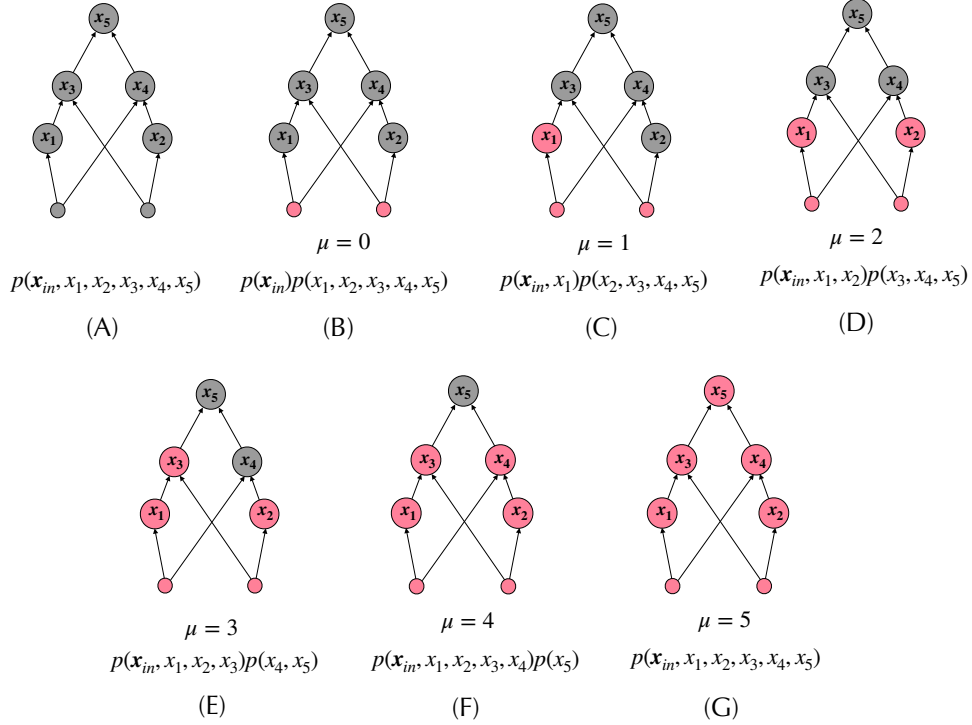


FIG. 3. Evolution of joint distribution under re-initialization of inputs and re-running the circuit gate-by-gate. (A) After a complete run, the joint distribution reflects maximal correlation among all gates. This correlation arises from the initial input distribution and the network of dependencies within the circuit. (B) In the next run, the input nodes are re-sampled from the input distribution $p(\mathbf{x}_{\text{in}})$, making the new inputs independent of the states of non-input gates from the previous run. As a result, the joint distribution after re-initialization is factored as $p(\mathbf{x}_{\text{in}})p(x_1, \dots, x_5)$, indicating that inputs and non-input gates are now statistically independent. (C) When gate x_1 updates based on the newly re-sampled input values, it becomes correlated with the input nodes while simultaneously losing correlation with the rest of the gates. Consequently, the joint distribution evolves to $p(\mathbf{x}_{\text{in}}, x_1)p(x_2, \dots, x_5)$. Similarly, (D), (E), (F), and (G) illustrate the sequential updates of the remaining gates and the corresponding evolution of the distribution. In particular, (G) demonstrates that after a complete run of the circuit, the distribution returns to its initial form as shown in (A).

Fig. 2). Once the input nodes are assigned new values, each gate updates sequentially in the prescribed topological order, with gate μ updating based on the values of its parent gates. After one complete execution, the output gates provide the final result corresponding to the given input, and moreover, the circuit is fed with new input values for the next run while all gate values remain unchanged. The same sequence of updates is repeated, with gates updating in topological order based on the new inputs and the latest values of their parents.

Due to this repeated use of the circuit, the probability distribution over the state of the circuit goes through a cycle, as depicted in Fig. 2 and Fig. 4 and explained below: after a complete execution of the circuit, the states of the gates are correlated with each other, as depicted in Fig. 2A. Importantly, the non-input gates are correlated with the input nodes. However, when new input values are assigned for the next execution, the input nodes become uncorrelated with the values of the non-input gates from the previous execution (Fig. 2B). Next, as the se-

quential process begins, and each gate updates its value based on the new values of its parents, there is a making and breaking of correlation. Before gate μ updates, it remains correlated with its children gates $\text{ch}(\mu)$ from the previous execution. However, since its parent gates $\text{pa}(\mu)$ have already been updated in the current execution, μ is not correlated with them at this stage. When gate μ updates, two simultaneous changes occur: first, μ becomes correlated with its parent gates $\text{pa}(\mu)$ in the current execution, and second, its new value becomes independent of the values of its children gates $\text{ch}(\mu)$ from the previous execution.

We assume input values are jointly sampled from an input distribution $p_{\text{in}}(\mathbf{x}_{\text{in}})$. We assume each run of the circuit is evaluated on the entire input distribution $p_{\text{in}}(\mathbf{x}_{\text{in}})$. The dependency of a gate on its parents is expressed by the conditional distribution $\pi_{\mu}(\mathbf{x}_{\mu}|\mathbf{x}_{\text{pa}(\mu)})$ for each non-input gate $\mu \in V_{\text{nin}}$. The conditional distributions π_{μ} together specify the conditional probability of the state of the non-input gates given the states of input gates:

$$R(\mathbf{x}_{\text{nin}}|\mathbf{x}_{\text{in}}) = \prod_{\mu \in V/V_{\text{in}}} \pi_{\mu}(\mathbf{x}_{\mu}|\mathbf{x}_{\text{pa}(\mu)}) \quad (5)$$

Note that, regardless of the gate being deterministic or noisy, since the inputs are randomly sampled from an input distribution p_{in} , the state of each gate, and hence the joint state of the circuit is a random variable. After the end of a complete run and before the beginning of the next run, the joint state of the entire circuit has a following probability distribution (see Fig. 3A)

$$p^0(\mathbf{x}) = R(\mathbf{x}_{\text{nin}}|\mathbf{x}_{\text{in}})p_{\text{in}}(\mathbf{x}_{\text{in}}) \quad (6)$$

1. Notation

We use $p^{\mu}(\mathbf{x})$ to denote the distribution over the joint state of the circuit **before the execution of gate μ** and after the execution of gate $\mu - 1$. Moreover, $p^0(\mathbf{x})$ denotes the distribution before the over-writing of new input values and $p^1(\mathbf{x})$ denotes the distribution after the over-writing of new input values but before gate $\mu = 1$ is executed.

For any given subset of nodes $\chi \subset V$, we define X_{χ} as the collection of random variables at the subset of nodes χ , and \mathbf{x}_{χ} as a particular set of values thereof; we denote $p_{\chi}(\mathbf{x}_{\chi})$ as the marginal distribution of X_{χ} , obtained from the maximally correlated joint distribution $p^0(\mathbf{x})$.

$$p_{\chi}(\mathbf{x}_{\chi}) = \sum_{\mathbf{x}_{V/\chi}} p^0(\mathbf{x}) \quad (7)$$

For example, we will use $\mathbf{x}_{:\mu}$ to denote the joint state of all nodes preceding gate μ , \mathbf{x}_{μ} to denote the state of gate μ and $\mathbf{x}_{\mu:}$ to denote the set of all nodes following gate μ . Accordingly, $p_{:\mu}$ denotes the marginal distribution over the joint state $\mathbf{x}_{:\mu}$ of gates preceding the gate μ obtained from $p^0(\mathbf{x})$.

$$p_{:\mu}(\mathbf{x}_{:\mu}) = \sum_{\mathbf{x}_{\mu}, \mathbf{x}_{\mu:}} p^0(\mathbf{x}) \quad (8)$$

Analogously, p_{in} and p_{nin} are used to denote the joint distribution over the states of input nodes and non-input gates respectively.

$$p_{\text{in}}(\mathbf{x}_{\text{in}}) = \sum_{\mathbf{x}_{\text{in}}} p^0(\mathbf{x}), \quad p_{\text{nin}}(\mathbf{x}_{\text{nin}}) = \sum_{\mathbf{x}_{\text{nin}}} p^0(\mathbf{x}). \quad (9)$$

A more comprehensive list of notation is provided in Table I.

2. Joint distribution after the re-initialization of the input nodes

As mentioned earlier, when the new inputs are initialized for the next run, the joint state of the non-input gates becomes independent of the new joint state of the input nodes (see Fig. 2B and Fig. 3B). Therefore, after the re-initialization of the input nodes, the joint distribution changes from $p^0(\mathbf{x})$,

$$p^1(\mathbf{x}) = p_{\text{in}}(\mathbf{x}_{\text{in}})p_{\text{nin}}(\mathbf{x}_{\text{nin}}). \quad (10)$$

Following this re-initialization, the non-input gates run sequentially and the distribution over the joint state evolves accordingly.

3. Joint distribution after the update of gate μ

Before gate μ updates, its state \mathbf{x}_{μ} is correlated with $\mathbf{x}_{\mu:}$ from the previous run of the circuit and it is uncorrelated with $\mathbf{x}_{:\mu}$ because of the new values. The joint distribution before the gate μ updates has the following form:

$$p^{\mu}(\mathbf{x}) = p_{:\mu}(\mathbf{x}_{:\mu})p_{\mu, \mu:}(\mathbf{x}_{\mu}, \mathbf{x}_{\mu:}). \quad (11)$$

After the update of the gate μ based on the new values of its parent gates, \mathbf{x}_{μ} becomes correlated with $\mathbf{x}_{:\mu}$ and independent with $\mathbf{x}_{\mu:}$ (see Fig. 3). Therefore,

$$p^{\mu+1}(\mathbf{x}) = p_{:\mu, \mu}(\mathbf{x}_{:\mu}, \mathbf{x}_{\mu})p_{\mu:}(\mathbf{x}_{\mu:}). \quad (12)$$

This transformation of probability distribution upon executing gate μ can be represented by

$$p(\mathbf{x}_{:\mu})p(\mathbf{x}_{\mu}, \mathbf{x}_{\mu:}) \rightarrow p(\mathbf{x}_{:\mu}, \mathbf{x}_{\mu})p(\mathbf{x}_{\mu:}). \quad (13)$$

Running gate μ correlates its output with its parents while making it conditionally independent of downstream variables. Intuitively, executing gate μ redistributes correlations: it introduces correlations between the gate's output and its parents, while breaking correlations with downstream variables. This type of redistribution of correlations occurs at each non-input gate as the circuit is evaluated in topological order, continually creating and erasing statistical dependencies among subsets of variables.

B. Mismatch cost of re-initializing inputs with new values.

During the process of overwriting new input values, the input nodes evolve independently of the rest of the

Table of notation	
Symbol	Definition
C_n	Circuit with input size n
μ	Index of a gate in circuit, $\mu \in \{1, 2, \dots, C_n \}$
$\text{pa}(\mu)$	Set of parent gates of gate μ
$\text{ch}(\mu)$	Set of children gates of gate μ
V	Set of input nodes and non-input gates in circuit
V_l	Set of gates in layer l of circuit
X_μ	Random variable representing the states of gate μ
X_l	Random variable representing the joint state of gates in layer l .
X_χ	Random variable representing the joint state of subset of gates χ .
\mathbf{x}	Joint state of the entire circuit
\mathbf{x}_μ	State of gate μ
$\mathbf{x}_{\text{pa}(\mu)}$	Joint state of parent gates of μ
$\mathbf{x}_{:\mu}$	Joint state of gates preceding gate μ , including input nodes
$\mathbf{x}_{\mu:}$	Joint state of gates following gate μ
\mathbf{x}_{in}	Joint state of the inputs
\mathbf{x}_{nin}	Joint state of non inputs gates
$\mathbf{x}_{-\mu}$	Joint state of all gates except gate μ and the parents of gate μ
\mathbf{x}_l	Joint state of gates in layer l
$\mathbf{x}_{:l}$	Joint state of gates in layers preceding layer l
$p^0(\mathbf{x})$	Maximally correlated distribution over the circuit states at the start of a new run
$p^\mu(\mathbf{x})$	Distribution over states of circuit before gate μ runs in a gate-by-gate execution
$p^l(\mathbf{x})$	Distribution over states of circuit before layer l runs in a layer-by-layer execution
$p_\chi(\mathbf{x}_\chi)$	Marginal distribution of subset χ of gates obtained from $p^0(\mathbf{x})$
$p_{:\mu}(\mathbf{x}_{:\mu})$	Marginal distribution of subset of gates preceding gate μ
$p_{\mu:}(\mathbf{x}_{\mu:})$	Marginal distribution of subset of gates following gate μ
$p_l(\mathbf{x}_l)$	Marginal distribution of subset of gates in layer l obtained from $p^0(\mathbf{x})$
$q^\mu(\mathbf{x})$	Prior distributions of process of updating gate μ in circuit
$q^0(\mathbf{x})$	Prior distribution of the process of overwriting the inputs with new values
$\tilde{q}^\mu(\mathbf{x})$	Distribution obtained by evolving $q^\mu(\mathbf{x})$ as gate μ updates
$q_{\mu, \text{pa}(\mu)}(\mathbf{x}_\mu, \mathbf{x}_{\text{pa}(\mu)})$	Prior distribution associated with gate μ
$\tilde{q}_{\mu, \text{pa}(\mu)}(\mathbf{x}_\mu, \mathbf{x}_{\text{pa}(\mu)})$	Distribution obtained by evolving $q_{\mu, \text{pa}(\mu)}(\mathbf{x}_\mu, \mathbf{x}_{\text{pa}(\mu)})$ under the update of gate μ
$q_{\text{pa}(\mu)}(\mathbf{x}_{\text{pa}(\mu)})$	Marginal distribution obtained from $q_{\mu, \text{pa}(\mu)}(\mathbf{x}_\mu, \mathbf{x}_{\text{pa}(\mu)})$
$q_{-\mu}(\mathbf{x}_{-\mu})$	Distribution over states of all gates in circuit not including μ and $\text{pa}(\mu)$
\mathcal{B}	Basis of logic gates
q_g	Short hand for prior distribution associated with logic gate $g \in \mathcal{B}$
$\tilde{\mathcal{B}}$	Set of (g, q_g) for every gates $g \in \mathcal{B}$
q_g^{\min}	Probability of least likely state under distribution q_g
$I_\mu(X_\mu; X_{\text{ch}(\mu)})$	Mutual information between gate μ and its children $\text{ch}(\mu)$ with reference to distribution $p^\mu(\mathbf{x})$
$I_\mu(X_\mu; X_{\text{pa}(\mu)})$	Mutual information between gate μ and its parents $\text{ch}(\mu)$ with reference to distribution $p^\mu(\mathbf{x})$
$I_\mu(X_\mu; X_{\mu:})$	Mutual information between gate μ and all gates following μ with reference to distribution $p^\mu(\mathbf{x})$
\mathcal{MC}_μ	Mismatch cost of running gate μ in a circuit
\mathcal{MC}_l	Mismatch cost of running layer l in a circuit
$\mathcal{MC}_{ow}(p_{in})$	Mismatch cost of overwriting inputs with input distribution p_{in}
$\mathcal{MC}(C_n, p_{in})$	Total mismatch cost of running the circuit C_n for the input distribution p_{in}

TABLE I. Table of notation for the main symbols used in the paper.

non-input nodes which remain unchanged. Therefore, updating input nodes with new values is a sub-system process where the sub-system \mathbf{x}_{in} evolves independently of \mathbf{x}_{nin} while the latter remains unchanged. For such a sub-system process, the prior distribution is product distribution, expressed as $q_0(\mathbf{x}_{\text{in}}, \mathbf{x}_{\text{nin}}) = q_0(\mathbf{x}_{\text{in}})q_0(\mathbf{x}_{\text{nin}})$ (see App. A 1). Since new values of the input nodes are sampled from $p_{\text{in}}(\mathbf{x}_{\text{in}})$, this prior distribution evolves to $\tilde{q}_0(\mathbf{x}_{\text{in}}, \mathbf{x}_{\text{nin}})p_{\text{in}}(\mathbf{x}_{\text{in}})q_0(\mathbf{x}_{\text{nin}})$.

$$q_{\text{in}}(\mathbf{x}_{\text{in}})q_{\text{nin}}(\mathbf{x}_{\text{nin}}) \longrightarrow p_{\text{in}}(\mathbf{x}_{\text{in}})q_{\text{nin}}(\mathbf{x}_{\text{nin}}) \quad (14)$$

while the actual distribution evolves from $p^0(\mathbf{x})$ to $p_{\text{in}}(\mathbf{x}_{\text{in}})p_{\text{nin}}(\mathbf{x}_{\text{nin}})$:

$$p^0(\mathbf{x}_{\text{in}}, \mathbf{x}_{\text{nin}}) \longrightarrow p_{\text{in}}(\mathbf{x}_{\text{in}})p_{\text{nin}}(\mathbf{x}_{\text{nin}}) \quad (15)$$

Since new input values are totally independent of the states of the rest of the gates, $I_1(\mathbf{x}_{\text{in}}; \mathbf{x}_{\text{nin}}) = 0$, and the drop in mutual information is

$$\Delta I(\mathbf{X}_{\text{in}}; \mathbf{X}_{\text{nin}}) = I_0(\mathbf{X}_{\text{in}}; \mathbf{X}_{\text{nin}}) - I_1(\mathbf{X}_{\text{in}}; \mathbf{X}_{\text{nin}}) \quad (16)$$

$$= I_0(\mathbf{X}_{\text{in}}; \mathbf{X}_{\text{nin}}) \quad (17)$$

Using Eq. (14) and (15), the mismatch cost of overwriting the input values evaluates to

$$\mathcal{MC}_{ow} = D(p^0||q^0) - D(p^1||\tilde{q}^0) \quad (18)$$

$$= I_0(\mathbf{X}_{\text{in}}; \mathbf{X}_{\text{nin}}) + D(p_{\text{in}}||q_{\text{in}}), \quad (19)$$

where the mutual information term $I_0(\mathbf{X}_{\text{in}}; \mathbf{X}_{\text{nin}})$ arises because the circuit begins each run in a correlated state: the values stored in the non-input nodes reflect remnants of the previous computation and are therefore statistically dependent on the previous inputs. When the input nodes are re-initialized with fresh values drawn from the new input distribution, these correlations are erased. As a result, the joint distribution over input and non-input

nodes becomes a product distribution at the start of the new run, and the loss of these pre-existing correlations results in a term $I_0(\mathbf{X}_{\text{in}}; \mathbf{X}_{\text{nin}})$ from the change in KL-divergence.

C. Mismatch cost of gate-by-gate or layer-by-layer implementation of the circuit.

We use $q^\mu(\mathbf{x})$ for the prior distributions associated with the process of updating the gate μ . Additionally, $q^0(\mathbf{x})$ is used to denote the prior associated with the process of overwriting. When \mathbf{x}_μ is updated based on the values of its parents $\mathbf{x}_{\text{pa}(\mu)}$, the rest of the nodes are unchanged. This makes it a subsystem process where \mathbf{x}_μ and $\mathbf{x}_{\text{pa}(\mu)}$ form a subsystem. The prior distribution therefore is a product distribution of the form

$$q^\mu(\mathbf{x}) = q_{\mu, \text{pa}(\mu)}(\mathbf{x}_\mu, \mathbf{x}_{\text{pa}(\mu)})q_{-\mu}(\mathbf{x}_{-\mu}) \quad (20)$$

When gate μ changes its state based on its parents states, the associated prior distribution $q_{\mu, \text{pa}(\mu)}(\mathbf{x}_\mu, \mathbf{x}_{\text{pa}(\mu)})$ evolves to $\tilde{q}_{\mu, \text{pa}(\mu)}(\mathbf{x}_\mu, \mathbf{x}_{\text{pa}(\mu)}) = \pi_\mu(\mathbf{x}_\mu|\mathbf{x}_{\text{pa}(\mu)})q_{\text{pa}(\mu)}(\mathbf{x}_{\text{pa}(\mu)})$, where $q_{\text{pa}(\mu)}(\mathbf{x}_{\text{pa}(\mu)})$ is the marginal distribution of $\text{pa}(\mu)$ obtained from $q_{\mu, \text{pa}(\mu)}(\mathbf{x}_\mu, \mathbf{x}_{\text{pa}(\mu)})$. Since the rest of the gates do not change when gate μ is updated, the distribution $q^\mu(\mathbf{x})$ evolves to $\tilde{q}^\mu(\mathbf{x})$, given by:

$$\tilde{q}^\mu(\mathbf{x}) = \tilde{q}_{\mu, \text{pa}(\mu)}(\mathbf{x}_\mu, \mathbf{x}_{\text{pa}(\mu)})q_{-\mu}(\mathbf{x}_{-\mu}). \quad (21)$$

The mismatch cost of updating the gate μ is given by,

$$\mathcal{MC}_\mu = D(p^\mu||q^\mu) - D(p^{\mu+1}||\tilde{q}^\mu) \quad (22)$$

Using expressions (11) and (12) for the actual probability distributions, and (20) and (21) for the prior distributions, the expressions for the mismatch cost \mathcal{MC}_μ becomes

$$\mathcal{MC}_\mu = S_{\mu+1}(X) - S_\mu(X) + I_{\mu+1}(X_\mu; X_{\text{pa}(\mu)}) + D(p_\mu p_{\text{pa}(\mu)}||q_{\mu, \text{pa}(\mu)}) - D(p_{\text{pa}(\mu)}||q_{\text{pa}(\mu)}), \quad (23)$$

where $I_{\mu+1}(X_\mu; X_{\text{pa}(\mu)})$ denotes the mutual information between μ and $\text{pa}(\mu)$ after the gate μ is updated. $S_\mu(X)$ and $S_{\mu+1}(X)$ are the entropy of the joint system (the entire circuit) before and after updating gate μ . The derivation of Eq. (23) is provided in App. A 3. More

importantly, the total mismatch cost of the entire circuit, given by the sum of mismatch cost of overwriting of inputs (Eq. 19) and mismatch cost running all gates sequentially, turns out to have the following form:

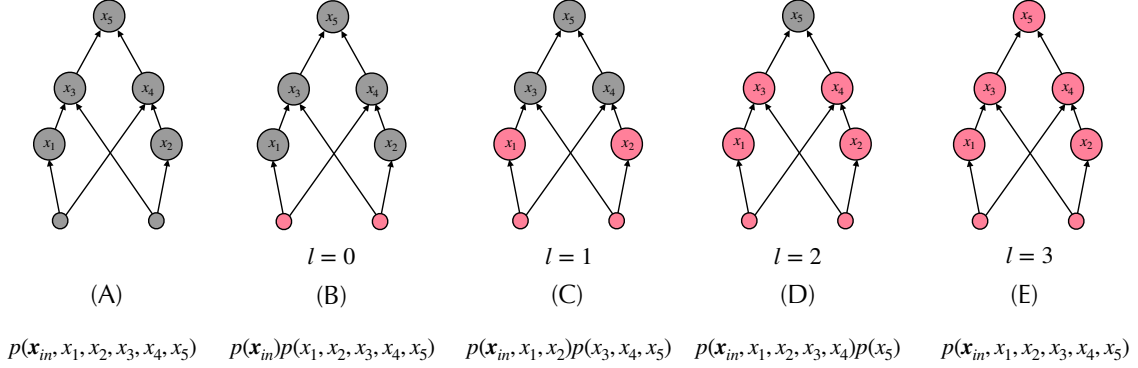


FIG. 4. Layer-by-layer implementation of a circuit. (A) State of the circuit after a complete run. (B) Updating of input nodes for the next run, with values re-sampled from $p(\mathbf{x}_{in})$. (C) The first layer consists of gates x_1 and x_2 . As they update together based on the newly sampled input values, they become correlated with the input nodes while losing correlation with the rest of the gates. Consequently, the joint distribution evolves to $p(\mathbf{x}_{in}, x_1, x_2)p(x_3, x_4, x_5)$. (D) Gates x_3 and x_4 make up layer 2. As they update based on the new values of gates x_1 and x_2 , they become correlated with them and the input nodes, while becoming independent of the state of x_5 . The distribution then evolves to $p(\mathbf{x}_{in}, x_1, \dots, x_4)p(x_5)$. Finally, in (E), gate x_5 , constituting layer 3, is updated, and the distribution returns to its initial form as shown in (A).

$$\mathcal{MC}(C_n, p_{in}) = \mathcal{MC}_{ow}(p_{in}) + \sum_{\mu \in V_{nin}} \mathcal{MC}_{\mu} \quad (24)$$

$$= D(p_{in} || q_{in}) + \sum_{\mu \in V_{nin}} I_{\mu+1}(X_{\mu}; X_{pa(\mu)}) + \sum_{\mu \in V_{nin}} [D(p_{\mu} p_{pa(\mu)} || q_{\mu, pa(\mu)}) - D(p_{pa(\mu)} || q_{pa(\mu)})]. \quad (25)$$

A few remarks about Eq. (25) are in order. In particular, the expression for the MMC of a single gate μ in Eq. (23) involves the entropy of the full circuit state, which is a global quantity. However, when these contributions are summed over all non-input gates, the intermediate entropy terms telescope and cancel. What remains are only the boundary terms,

$$S_1(\mathbf{X}) - S_{|V_{nin}|+1}(\mathbf{X}), \quad (26)$$

corresponding to the entropy of the joint circuit state immediately after the inputs are re-initialized and before any non-input gates are executed, and the entropy after all non-input gates have completed their updates. This boundary contribution can be written as

$$S_1(\mathbf{X}) - S_{|V_{nin}|+1}(\mathbf{X}) = -I_0(X_{in}; X_{nin}), \quad (27)$$

reflecting the correlations established between inputs and non-input nodes during the computation. Consequently, after adding the overwriting MMC in Eq. (19), the total mismatch cost simplifies to the expression in Eq. (25).

It is straightforward to extend the analysis for a layer-by-layer implementation of circuit (see Fig. 4). Based on a topological ordering of a DAG, it is possible to stratify

the set of gates in a natural way into layers. Starting from the set of input nodes

$$V_0 := \mu \in V : pa(\mu) = \emptyset, \quad (28)$$

we define the l -th layer recursively by

$$V_l := \left\{ \mu \in V \setminus \bigcup_{k=0}^{l-1} V_k : pa(\mu) \subseteq \bigcup_{k=0}^{l-1} V_k \right\}. \quad (29)$$

This construction assigns each gate to the earliest layer in which all of its parents have already been evaluated, thereby inducing a valid feedforward layering of the circuit.

Let X_l be the random variable denoting the joint state of gates in layer l and let \mathbf{x}_l denote a value of X_l . In a layer-by-layer implementation, all the gates in a layer are updated simultaneously. Let d be the number of layers in the circuit. Then, analogous to Eq. (25), the total mismatch cost of running all non-input layers is given

by,

$$\begin{aligned} \mathcal{MC}_{ow} + \sum_{l=1}^d \mathcal{MC}_l &= D(p_{in}||q_{in}) + \sum_{l=1}^d I_{l+1}(X_l; X_{pa(l)}) \\ &+ \sum_{l=1}^d [D(p_l p_{pa(l)}||q_{l,pa(l)}) - D(p_{pa(l)}||q_{pa(l)})], \end{aligned} \quad (30)$$

where p_l , $p_{pa(l)}$, $q_{l,pa(l)}$, and $q_{pa(l)}$ are defined for layer l and have their usual meaning as in Eq. (25).

Updating multiple gates simultaneously in a layer-by-layer approach, instead of updating gates sequentially one by one, represents a form of time-coarse graining. This is because grouping several updates into a single time step effectively reduces the temporal resolution of the system's dynamics. As demonstrated in [17], mismatch cost decreases under time-coarse graining. Applied to circuits, this result implies that the mismatch cost of a layer-by-layer implementation always serves as a lower bound on the mismatch cost of a gate-by-gate implementation. In Fig. 5, we compare the mismatch costs of layer-by-layer and gate-by-gate implementations of a ripple-carry adder. Gate-by-gate mismatch cost is computed using Eq. (25), while the layer-by-layer mismatch cost is computed using Eq. (30). As a consequence of the lowering in mismatch cost under time-coarse graining, the layer-by-layer mismatch cost is lower than the gate-by-gate mismatch cost across ripple-carry adder circuits with varying input lengths.

Additionally, note that as the computation in a circuit progress—whether gate-by-gate or layer-by-layer—the distribution over the states cycles through a sequence of distributions (see Fig. 3 and 4). It is important to emphasize that, for the calculation of the total mismatch cost, when calculating the total mismatch cost, the phase at which the sequence of distributions is started does not impact the final mismatch cost, as long as the full cycle of execution is completed.

Moreover, the sequence of gate implementations in a circuit can be modeled as a periodic process. In practical computational devices based on circuits, the execution of gates or layers is typically driven by a clock [19]. From this perspective, the process is periodic, with gates executed at each clock cycle, sequentially leading to the completion of the full circuit. In Appendix B 3, we present the MMC calculation for this clock-driven model of circuit execution. This approach yields the same expression for the MMC as given in Eq. (22).

In the next section, we use Eq (25) to calculate the mismatch cost of various circuit families and broadly investigate how does the circuit structure affect their mismatch cost. In particular, we define mismatch cost complexity, analogous to the size and depth complexity of a circuit family. We will then establish results that relate mismatch cost complexity to size complexity.

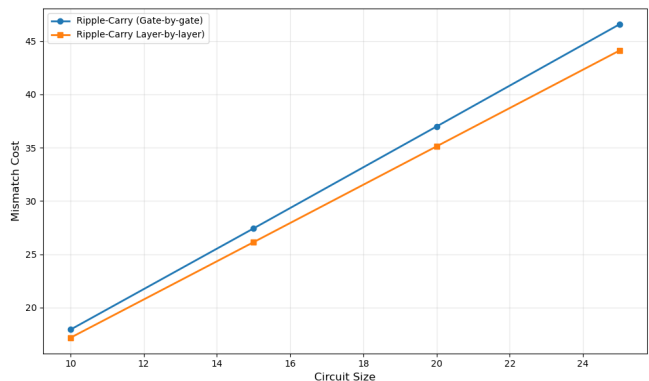


FIG. 5. Comparison of layer-by-layer and gate-by-gate mismatch costs for the ripple-carry adder circuit family. Notably, the layer-by-layer mismatch cost remains consistently lower than the gate-by-gate mismatch cost. In this comparison, the input distribution is uniformly random for both implementations, and the priors of all gates in the circuits are also uniform.

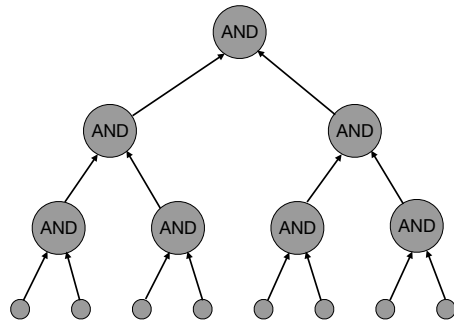


FIG. 6. Binary tree of AND gates. The size of the grows as n for n input nodes whereas its depth grows as $\log(n)$.

IV. THE MISMATCH COST COMPLEXITY OF A CIRCUIT FAMILY

We aim to explore the relationship between the total mismatch cost of a circuit and other complexity measures, such as size and depth. To this end, we extend the definition of a basis for a circuit family to include the prior distribution associated with each logic gate in the basis. For a given basis \mathcal{B} , we define the *associated prior basis* $\tilde{\mathcal{B}} = \{(g, q_{g,pa(g)}) : g \in \mathcal{B}\}$, where $q_{g,pa(g)}$ denotes the prior distribution associated with gate $g \in \mathcal{B}$. The definition of extended prior basis allows us to define mismatch cost complexity associated with a circuit family.

Definition 3 (Mismatch Cost Complexity) *Given a basis \mathcal{B} and an associated prior basis $\tilde{\mathcal{B}}$, a circuit family $\{C_n\}_{n \in \mathbb{N}}$ is said to have mismatch cost complexity $m(n)$, where $m : \mathbb{N} \rightarrow \mathbb{R}^+$, if its mismatch cost is uniformly*

bounded in the worst case over input distributions, i.e.,

$$\mathcal{MC}(C_n, p_{\text{in}}) \leq m(n) \quad (31)$$

for all input distributions p_{in} and all $n \in \mathbb{N}$.

Analogously, we define the mismatch cost complexity class of functions:

Definition 4 (Mismatch cost complexity class)

Let $m : \mathbb{N} \rightarrow \mathbb{R}^+$. For a given associated prior basis $\tilde{\mathcal{B}}$, $\text{MMC}(m)$ is the class of functions f for which there exist a circuit family \mathcal{C} of mismatch cost complexity m .

The mismatch cost complexity associated with any circuit family is influenced by several key properties of the circuit. For example, it depends on the basis $\tilde{\mathcal{B}}$, which includes the types of logic gates allowed in the circuit and their associated prior distribution. Moreover, the topology of the circuit, in combination with the input distribution, jointly determines the mutual information $I_{\mu+1}(X_\mu; X_{\text{pa}(\mu)})$, which contributes to the mismatch cost for each gate μ (see Eq. (25)). Additionally, the topology and input distribution together determine the distributions $p_\mu(\mathbf{x}_\mu)$ and $p_\mu(\mathbf{x}_{\text{pa}(\mu)})$ for each gate μ .

With these definitions we can derive the following result:

Theorem 1 Suppose that:

- (a) For every gate μ in the circuit, the prior distribution over μ and its parents $\text{pa}(\mu)$ factorizes as a product distribution; $q_{\mu, \text{pa}(\mu)}(\mathbf{x}_\mu, \mathbf{x}_{\text{pa}(\mu)}) = q_\mu(\mathbf{x}_\mu)q_{\text{pa}(\mu)}(\mathbf{x}_{\text{pa}(\mu)})$
- (b) All gates share the same marginal prior, i.e., $q_\mu = q_g$ for all gate types g ,
- (c) The prior distribution over the n -input nodes $(x_{\text{in},1} \dots x_{\text{in},n})$ is also a product distribution; $q_{\text{in}}(\mathbf{x}_{\text{in}}) = \prod_{k=1}^n q_i(x_{\text{in},k})$

Then the total mismatch cost of running the circuit C_n , in the worst case over input distributions, satisfies the upper bound

$$\mathcal{MC}(C_n) \leq |C_n| K + n K_{\text{in}}, \quad (32)$$

independently of the fan-in and fan-out of the gates, where

$$K = \log\left(\frac{1}{q_g^{\min}}\right), \quad K_{\text{in}} = \log\left(\frac{1}{q_i^{\min}}\right)$$

are positive constants determined by the minimal components of the gate and input node priors, respectively.

The proof of Theorem 1 is provided in (B1). We refer to a basis in which all the logic gates have identical prior distributions as a *homogeneous associated prior*

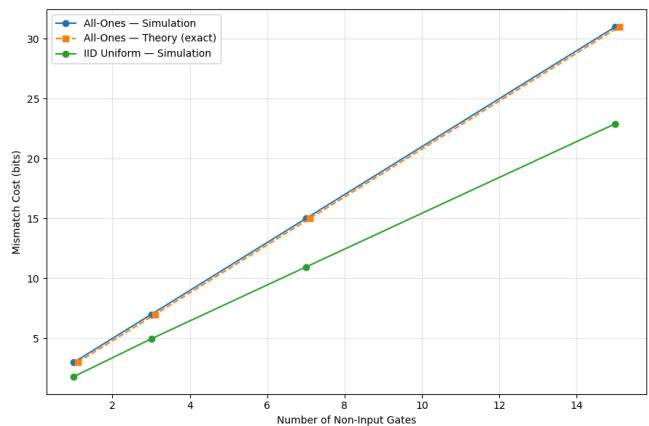


FIG. 7. Saturating the Upper Bound on MMC for the AND Binary Tree Circuit Family. The solid blue line represents the total mismatch cost obtained by using Eq. (25) and a prior that is uniform for an input distribution consisting entirely of all ones, matching exactly with the orange dashed line, which corresponds to the theoretical upper bound given by Eq. (32). In contrast, when the input distribution is a uniform distribution, the actual total mismatch cost of AND binary tree remains consistently lower than the theoretical upper bound: the solid green line depicts the total mismatch cost for a uniform input distribution.

basis. Thm. (1) establishes a relationship between the size complexity and the mismatch cost complexity of any circuit family constructed from gates in a homogeneous prior basis. If $s(n)$ denotes the size complexity of the circuit family, then according to Eq. (32), the mismatch cost complexity $m(n)$ of the circuit family is given by:

$$m(n) \leq s(n) K + n K_{\text{in}}, \quad (33)$$

According to Eq. (33), if the size complexity $s(n)$ of a circuit family grows as a polynomial function of the input size, then the upper bound on the mismatch cost complexity for any homogeneous prior basis also scales polynomially with the input size. In other words, any Boolean function that can be implemented by a polynomial-size circuit can also be realized by a circuit family whose mismatch cost complexity does not exceed polynomial growth. This observation leads to the following corollary:

Corollary 1.1 For any given basis \mathcal{B} and any associated homogeneous prior basis $\tilde{\mathcal{B}}$,

$$\mathbf{P}_{/\text{poly}} \subseteq \text{MMC}(\text{poly}) \quad (34)$$

It remains an open question whether the converse holds—that is, whether any function implementable by a circuit family with a mismatch cost that grows no faster than polynomial can also be realized by a circuit family whose size complexity is polynomial bounded, and thus whether $\mathbf{P}_{/\text{poly}} = \text{MMC}(\text{poly})$.

The worst-case upper bound in Theorem 1 can be saturated for certain circuit families with certain (worst-case) input distributions. For example, consider the circuit family consisting of AND binary tree. The number of gates in a binary tree with input n is $|C_n| = n$. Therefore, according to Eq. (32), an upper bound on the MMC is

$$\mathcal{MC}(C_n) \leq n \log \left(\frac{1}{q_{\min}} \right) + n \log \left(\frac{1}{q_i^{\min}} \right) \quad (35)$$

As shown in Fig. 7, when the input is always all ones, the theoretical upper bound is fully attained by the actual total MMC of the circuit. However, for other input distributions, such as a uniform input distribution, the upper bound is not saturated, and the actual total mismatch cost remains consistently lower than the theoretical upper bound.

Next, we examine the scenario where the prior distribution is not homogeneous across the logic gates in the basis, i.e., when assumption (b) of Thm. (1) no longer holds. For a given basis \mathcal{B} , we denote the prior distribution associated with each gate $g \in \mathcal{B}$ by q_g . The following result tells you how the mismatch cost complexity varies with input size for an inhomogeneous prior basis:

Theorem 2 For a given basis \mathcal{B} , let $\{C_n\}_{n \in \mathbb{N}}$ be circuit family and let $\tilde{\mathcal{B}} = \{(g, q_g) | g \in \mathcal{B}\}$ be the associated prior basis. Then, the mismatch cost of circuit of input size n is upper bounded by,

$$\mathcal{MC}(C_n, p_{\text{in}}) \leq \sum_{g \in \mathcal{B}} \#_g(n) K_g + n K_{\text{in}}. \quad (36)$$

where $\#_g(n)$ is the number of gates of type g in C_n and $K_g = \log(1/q_g^{\min})$.

The proof is provided in App. B2. Note that Thm. (2) provides a slight generalization of Thm. (1) and applies when different logic gates have different priors. Several key aspects distinguish it from the homogeneous prior case. For instance, in the homogeneous prior setting, the worst-case upper bound on the mismatch cost is always proportional to the size complexity $|C_n|$ of the circuit family for every n . However, with heterogeneous priors, this proportionality may no longer hold.

To illustrate this, consider a circuit family $\{C_n\}_{n \in \mathbb{N}}$ whose basis comprises two types of gates — say, AND and XOR — labeled as 1 and 2. Assume that the number of AND gates in this circuit family scales as $\#_1(n) = \log(n)$, while the number of XOR gates scales as $\#_2(n) = n^3$. According to Thm. (2), the upper bound on the mismatch cost is given by:

$$\begin{aligned} \sum_{g \in \mathcal{B}} \#_g(n) K_g + n K_{\text{in}} &= \#_1(n) K_1 + \#_2(n) K_2 + n K_{\text{in}} \\ &= \log(n) K_1 + n^3 K_2 + n K_{\text{in}} \end{aligned} \quad (37)$$

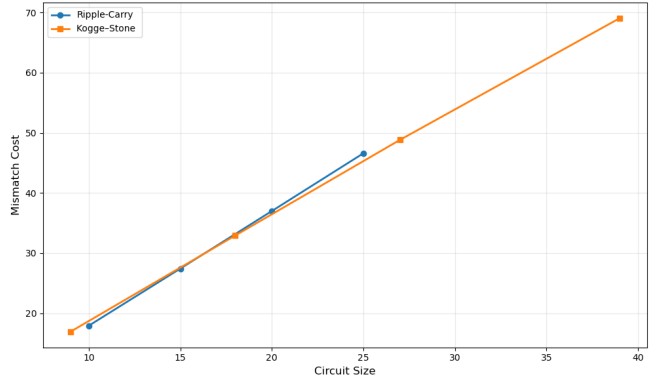


FIG. 8. The MMC of two different circuit families implementing the addition function, which takes two integers in the standard n -bit representation and returns their sum in the standard $(n + 1)$ -bit representation.

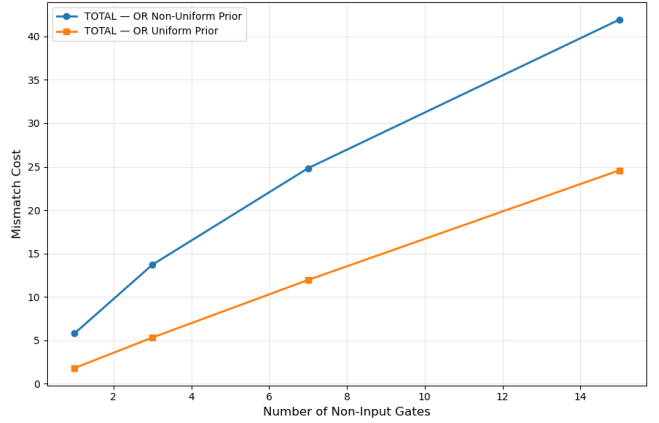


FIG. 9. Mismatch cost scaling for a circuit family with homogeneous (orange) vs. heterogeneous priors (blue). The circuit family that we consider here consist of binary tree made up of AND and OR gates; each layer had one OR gate and rest of the gates are AND. The solid blue curve shows the mismatch cost when the prior of OR gates differs from the uniform prior of AND gates (heterogeneous priors). For the case where AND and OR gates have different prior distribution, the mismatch cost is not linear with circuit size (Thm. (2)). In contrast, the orange line represents the mismatch cost for the same circuit family with identical priors for OR and AND gates (homogeneous priors), and the mismatch cost scales linearly with the circuit size.

Now, suppose the priors associated with these two types of gates are such that $K_1 \gg K_2$ and $K_1 \gg K_{\text{in}}$. This can arise, for example, when $q_1^{\min} < q_2^{\min}$. Under this condition, for small n , the upper bound on the mismatch cost scales as $\log(n)$. However, as n grows large, n^3 becomes the dominant term. This example demonstrates how, in the case of heterogeneous priors, the MMC can scale differently from the size complexity of the circuit family.

In Fig. 9, we illustrate how heterogeneous prior dis-

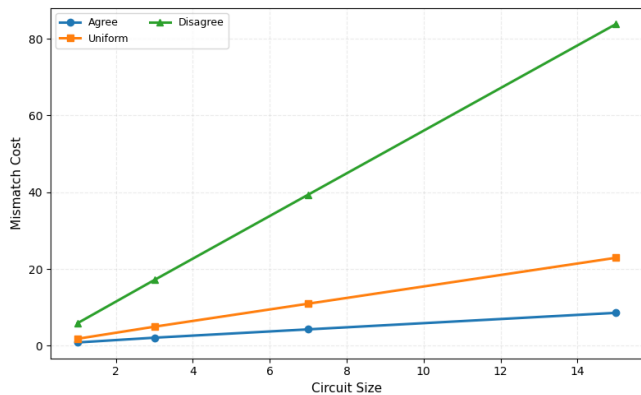


FIG. 10. Mismatch cost for a family of binary-tree AND circuits under different gate priors. For a uniform input distribution, the evaluation of the circuit induces a joint distribution over output \mathbf{x}_g and inputs $\mathbf{x}_{\text{pa}(g)}$ of each gate g . The figure shows the total mismatch cost for three choices of the gate prior $q_g(\mathbf{x}_g, \mathbf{x}_{\text{pa}(g)})$: (blue) a prior ‘agreeing’ to the ideal AND behavior, assigning 97% probability to the correct AND output given the inputs; (orange) a uniform prior over the joint input–output states; (green) a prior that assigns 97% probability to the output opposite to that of an ideal AND gate (‘disagreeing’ with the ideal AND behavior). The comparison illustrates how agreement or disagreement between the prior and the actual gate behavior impacts the total mismatch cost.

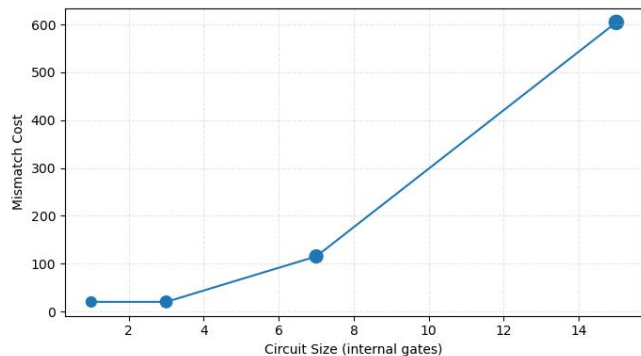


FIG. 11. Mismatch cost of a mixed binary tree circuit family. This figure illustrates that the linear cost–size relation need not hold for circuit families in the finite input regime. The circuit family is constructed as follows: starting with depth-1 tree which consists of an AND gate, the depth-2 tree is made of CONST gates that always output zero, depth-3 tree made from NAND gates and lastly, depth 4 tree is a tree of OR gates. All gates are evaluated under the same prior: inputs are assumed independent and uniformly distributed, so that $q_{\text{pa}(g)}(\mathbf{x}_{\text{pa}(g)}) = \frac{1}{4}$ for all $\mathbf{x}_{\text{pa}(g)} \in \{0, 1\}^2$, and $q_{g|\text{pa}(g)}(\mathbf{x}_g | \mathbf{x}_{\text{pa}(g)}) = \begin{cases} 1 - \varepsilon & \text{if } g = x \wedge y, \\ \varepsilon & \text{otherwise,} \end{cases}$ with $\varepsilon = 10^{-12}$. This means that the prior strongly favors AND behavior, and deviations from AND incur mismatch cost. Jointly, $q_{\text{pa}(g)}$ and $q_{g|\text{pa}(g)}$ determine the prior $q_{g, \text{pa}(g)}(\mathbf{x}_g, \mathbf{x}_{\text{pa}(g)}) = q_{g|\text{pa}(g)}(\mathbf{x}_g | \mathbf{x}_{\text{pa}(g)})q_{\text{pa}(g)}(\mathbf{x}_{\text{pa}(g)})$.

tributions across gate types can lead to deviations from linear scaling of mismatch cost with circuit size. Specifically, Fig. 9 considers a family of binary-tree circuits composed of AND and OR gates, where each layer contains a single OR gate and the remaining gates are AND gates. The prior distributions for the AND gates are fixed to be uniform, while the prior assigned to the OR gates is allowed to vary. The figure compares two scenarios: one in which the OR gates share the same prior as the AND gates, and another in which the OR gates have a different prior. In the former case, the total MMC scales linearly with circuit size, whereas in the latter case this linear scaling is broken. This example illustrates how heterogeneity in gate priors alone—without any change in circuit topology—can induce deviations from linear MMC scaling.

V. APPLICATIONS TO CIRCUIT COMPLEXITY

The results derived so far have many implications for understanding the thermodynamic costs associated with computation in circuits, as well as for the broader concept of circuit complexity. In this section we briefly sketch a few of them.

A. MMC of different circuit families implementing the same function family

The problem of computing a Boolean function with a circuit family under resource constraints naturally leads to the challenge of optimizing both circuit size and depth complexity. Since a Boolean function can be computed by multiple circuit families, size and depth serve as key measures of computational efficiency. The goal, therefore, is to identify the most efficient circuit family—one that minimizes both size and depth complexity. While size complexity corresponds to space efficiency and depth complexity to time efficiency, mismatch cost complexity serves as a measure of thermodynamic efficiency—the minimal dissipated heat in a circuit. Thus, when comparing two circuit families computing the same Boolean function, mismatch cost is a key metric for evaluating thermodynamic efficiency.

For example, the Boolean function ADD^n , which computes the sum of two n -bit binary numbers (discussed in Sec. II A), can be implemented by two circuit families: the ripple-carry adder and the carry look-ahead adder. RCA has linear size and depth complexity, while CLA has size complexity of $n \log n$ and logarithmic depth complexity.

In Fig. 8, we compare the mismatch cost of RCA and CLA across various input sizes. The results show a linear scaling of mismatch cost with size complexity for both

circuits. However, as input size increases, RCA consistently exhibits a lower mismatch cost than CLA, indicating that despite being slower, RCA is thermodynamically more efficient.

B. Relationship between MMC complexity and size complexity

Theorems 1 and 2 provide an upper bound on the total mismatch cost (MMC) as a function of the number of gates in a circuit. This bound is worst-case over all input distributions, meaning it holds regardless of the specific inputs fed to the circuit.

The relationship between MMC and circuit size can be further explored under different choices of prior distributions. In the case of a *homogeneous prior basis*, all logical gates in the circuit share the same prior distribution. The particular choice of this prior determines the slope of the resulting linear relationship between MMC and circuit size. For instance, Fig. 10 shows the MMC for a fixed circuit family of AND binary trees under several prior distributions; as expected, the slope of the linear relationship changes with the prior.

It is important to note that the bounds in Theorem 1 are worst-case. In practice, the actual MMC may not scale linearly with circuit size for certain circuit families under specific input distributions. As an example, Fig. 11 illustrates a circuit family for which the MMC exhibits a highly non-linear dependence on circuit size.

Moreover, the assumption of a homogeneous prior is rarely realistic in practice. The physical implementation of a logic gate typically depends on its type; for example, an AND gate may involve different underlying physical processes than an XOR gate. Consequently, just like other physical characteristics of gates, the prior distribution naturally varies with gate type. This heterogeneity influences the thermodynamic cost of a circuit, as discussed above and illustrated in Fig. 9.

Fig. 12 demonstrates how the mismatch cost of individual logic gates changes as their prior distributions shift. In particular, the mismatch cost tends to increase as the prior deviates further from uniform. Similarly, Fig. 13 shows the impact of heterogeneous priors on the total MMC of a fixed circuit composed of AND and OR gates, highlighting how increasing disparity between gate priors can affect the overall thermodynamic cost.

C. Minimizing MMC or Minimizing circuit size for a given Boolean function?

Finding the smallest-size circuit for a given Boolean function is a central problem in circuit complexity and often involves optimizing for minimal redundancy. However, the circuit with the smallest size does not neces-

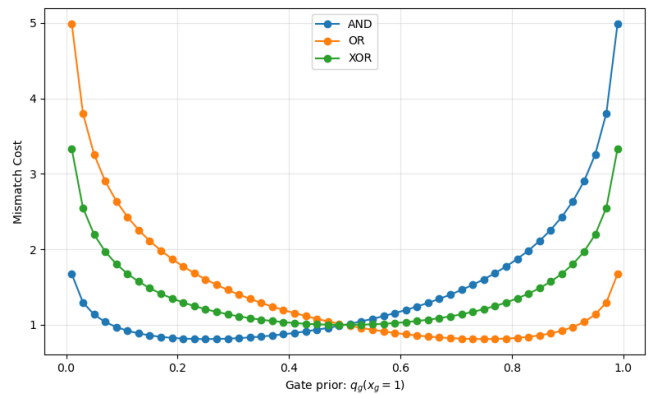


FIG. 12. Mismatch cost of individual gates as a function of their prior distributions. The input distribution to the gate is uniform. The x-axis represents the support of prior distribution at $x_g = 1$.

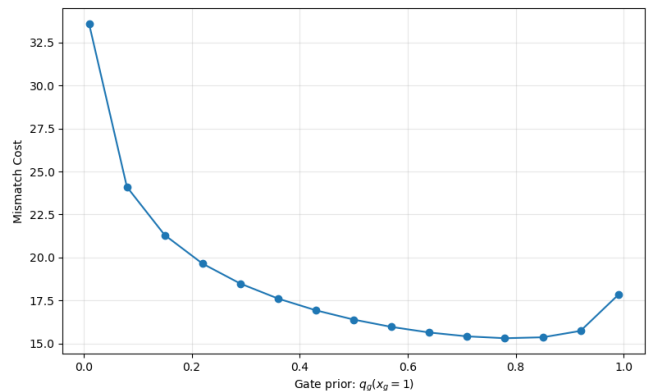


FIG. 13. Total mismatch cost of a circuit with 4 layers, each containing two AND gates and one OR gate. The prior distribution for AND gates is fixed and uniform, while the prior for OR gates is varied. The plot shows how the total mismatch cost changes with the OR gate prior.

sarily minimize total MMC. For instance, consider computing the NAND function: while it can be implemented with a single NAND gate, an alternative circuit using an AND gate followed by a NOT gate might result in a lower MMC if the NAND gate's prior is highly non-uniform, while the priors for AND and NOT are closer to uniform. This example illustrates that optimizing for thermodynamic cost may require different design choices than optimizing for size alone, and raises the broader question of trade-offs between logical and energetic efficiency in circuit design.

VI. DISCUSSION AND FUTURE WORK

Our work establishes a framework for analyzing the unavoidable thermodynamic costs of computation in Boolean circuits by deriving the expression for mismatch

cost. This formulation allows for a direct comparison between circuit families based on their mismatch cost complexity, providing a new perspective on circuit optimization—one that extends beyond minimizing size and depth to include energetic efficiency.

Our central technical result for Boolean circuits is Eq. (25), which provides a closed-form expression for the total MMC incurred when a circuit is run on a given input distribution. This expression applies equally to gate-by-gate execution and to layer-by-layer execution. Once the prior distributions associated with the gates are specified—capturing, at a coarse-grained and design-level assumptions about typical operating conditions—the total MMC becomes a circuit-level quantity that can be evaluated directly from the circuit’s architecture. In this sense, MMC is an unavoidable contribution to dissipation that is rooted fundamentally in the topology and modular organization of the circuit itself, together with the mismatch between the input statistics encountered in practice and those for which the circuit is effectively optimized.

Developed from Eq. 25, a key result of our study is Th. (1), which establishes an upper bound on the mismatch cost complexity that scales linearly with the size complexity of a circuit family under the assumption of a homogeneous prior distribution across all gates. Understanding precisely what causes the slope differences between circuit families, is still a question. In contrast to Th. (1), Th. (2) relaxes this assumption, allowing for cases where mismatch cost complexity deviates from size complexity. This result opens avenues for further exploration into how circuit structure, gate heterogeneity, and prior distributions influence thermodynamic costs. For example, with known prior distributions for each type of gate, a key question arises: how can we optimize the circuit topology associated with a Boolean function to minimize the thermodynamic cost?

Another key concept we introduce is mismatch cost complexity, which puts energetic cost on similar footing with more familiar resources like circuit size and depth. This lets us define corresponding mismatch cost complexity classes, which classifies computational problems according to whether they admit circuit families whose worst-case MMC grows no faster than some specified function. The motivation is very much in the spirit of standard complexity classes such as $\mathbf{P}_{/\text{poly}}$ or NC (Nick’s class), except that here the organizing principle is thermodynamic cost rather than purely combinatorial resources. This viewpoint opens up a new direction of thinking about computation that is grounded in physical resource constraints. For instance, we showed that $\mathbf{P}_{/\text{poly}} \subseteq \text{MMC}(\text{poly})$: any problem solvable by polynomial-size circuits can also be implemented by circuits whose worst-case mismatch cost grows at most polynomially. What we do not yet know is whether the converse holds—namely, whether polynomially bounded

MMC necessarily implies polynomial size, i.e., whether $\mathbf{P}_{/\text{poly}} = \text{MMC}(\text{poly})$. More broadly, the properties of mismatch cost complexity is still largely unexplored, and getting a better handle on it may shed new light on the energetic resource requirements of computation, beyond what size and depth alone can capture.

Another open question concerns the role of fan-in and fan-out—the number of inputs to, and outputs from, a gate, respectively—in determining the total mismatch cost. Fan-out greater than one allows the same gate output to be reused at multiple downstream locations, often reducing overall circuit size. However, it remains unclear how such logical reuse affects the minimal thermodynamic cost. Does increasing fan-out tend to reduce MMC, in analogy with its effect on size? Or might it leave MMC unchanged—or even increase it—by inducing additional correlations loss with each run? Understanding this trade-off between logical reuse and energetic dissipation is not an important theoretical question but it has direct implications for circuit architecture and hardware design. More generally, our observation that layer-by-layer execution yields a lower MMC than gate-by-gate execution suggests a practical design principle: to the extent possible, implementing gates simultaneously in synchronized, clocked layers may reduce thermodynamic overhead relative to more sequential execution. This points to a potential energetic advantage of highly parallel, clocked architectures, beyond their well-known benefits for latency and throughput.

Another fundamental problem is identifying the circuit family for a given Boolean function that minimizes mismatch cost. Understanding how this circuit family differs from those optimized for size or depth complexity would clarify the fundamental trade-offs between space, time, and thermodynamic cost in computation. Another intriguing direction is the thermodynamic analysis of circuit classes such as NC , which consists of functions that can be efficiently parallelized. A key open question is whether functions in NC —those that can be computed efficiently in parallel—are also implementable by circuits with low thermodynamic cost. Investigating this could provide new insights into the interplay between parallelizability and energetic efficiency in computation.

VII. ACKNOWLEDGMENT

This work was supported by the U.S. National Science Foundation (NSF) Grant 2221345. We thank the Santa Fe Institute for helping to support this research. We also thank Sosuke Ito, David Soloveichik and David Doty for helpful discussions.

-
- * Corresponding author: mahran.yousef2@gmail.com
- [1] Alan Mathison Turing et al. On computable numbers, with an application to the entscheidungsproblem. *J. of Math.*, 58(345-363):5, 1936.
 - [2] Michael O Rabin. Degree of difficulty of computing a function. *Tech. Rpt.*, (1), 1960.
 - [3] Stephen A Cook. An overview of computational complexity. *ACM Turing award lectures*, page 1982, 2007.
 - [4] Sanjeev Arora and Boaz Barak. *Computational complexity: a modern approach*. Cambridge University Press, 2009.
 - [5] Alan Cobham. The intrinsic computational difficulty of functions. 1965.
 - [6] Rolf Landauer. Irreversibility and heat generation in the computing process. *IBM journal of research and development*, 5(3):183–191, 1961.
 - [7] Charles H Bennett. The thermodynamics of computation—a review. *International Journal of Theoretical Physics*, 21:905–940, 1982.
 - [8] Christian Van den Broeck and Massimiliano Esposito. Ensemble and trajectory thermodynamics: A brief introduction. *Physica A: Statistical Mechanics and its Applications*, 418:6–16, 2015.
 - [9] Udo Seifert. Stochastic thermodynamics, fluctuation theorems and molecular machines. *Reports on progress in physics*, 75(12):126001, 2012.
 - [10] David H Wolpert. The stochastic thermodynamics of computation. *Journal of Physics A: Mathematical and Theoretical*, 52(19):193001, 2019.
 - [11] David H. Wolpert and Thomas E. Ouldridge. Thermodynamics of deterministic finite automata operating locally and periodically. *Physical Review E*, 109(2):024119, 2024.
 - [12] David H Wolpert, Jan Korbel, Christopher W Lynn, Farita Tasnim, Joshua A Grochow, Gülce Kardeş, James B Aimone, Vijay Balasubramanian, Eric De Giuli, David Doty, et al. Is stochastic thermodynamics the key to understanding the energy costs of computation? *Proceedings of the National Academy of Sciences*, 121(45):e2321112121, 2024.
 - [13] Heribert Vollmer. *Introduction to circuit complexity: a uniform approach*. Springer Science & Business Media, 1999.
 - [14] Artemy Kolchinsky and David H Wolpert. Dependence of integrated, instantaneous, and fluctuating entropy production on the initial state in quantum and classical processes. *Physical Review E*, 104(5):054107, 2021.
 - [15] Artemy Kolchinsky and David H Wolpert. Dependence of dissipation on the initial distribution over states. *Journal of Statistical Mechanics: Theory and Experiment*, 2017(8):083202, 2017.
 - [16] Gonzalo Manzano, Gülce Kardeş, Édgar Roldán, and David H Wolpert. Thermodynamics of computations with absolute irreversibility, unidirectional transitions, and stochastic computation times. *Physical Review X*, 14(2):021026, 2024.
 - [17] Abhishek Yadav, Francesco Caravelli, and David Wolpert. Mismatch cost of computing: from circuits to algorithms. *arXiv preprint arXiv:2411.16088*, 2024.
 - [18] Mark Horowitz. 1.1 computing’s energy problem (and what we can do about it). In *2014 IEEE International Solid-State Circuits Conference Digest of Technical Papers (ISSCC)*, page 10–14. IEEE, February 2014.
 - [19] Neil HE Weste and David Harris. *CMOS VLSI design: a circuits and systems perspective*. Pearson Education India, 2015.
 - [20] Thomas N Theis and H-S Philip Wong. The end of moore’s law: A new beginning for information technology. *Computing in science & engineering*, 19(2):41–50, 2017.
 - [21] Eric Masanet, Arman Shehabi, Nuo Lei, Sarah Smith, and Jonathan Koomey. Recalibrating global data center energy-use estimates. *Science*, 367(6481):984–986, 2020.
 - [22] Anantha P Chandrakasan and Robert W Brodersen. Minimizing power consumption in digital cmos circuits. *Proceedings of the IEEE*, 83(4):498–523, 2002.
 - [23] Abdellatif Bellaouar and Mohamed Elmasry. *Low-power digital VLSI design: circuits and systems*. Springer Science & Business Media, 2012.
 - [24] Clyde P Kruskal, Larry Rudolph, and Marc Snir. A complexity theory of efficient parallel algorithms. *Theoretical Computer Science*, 71(1):95–132, 1990.
 - [25] Gülce Kardeş and David Wolpert. Inclusive thermodynamics of computational machines. *arXiv preprint arXiv:2206.01165*, 2022.
 - [26] Philipp Strasberg, Javier Cerrillo, Gernot Schaller, and Tobias Brandes. Thermodynamics of stochastic turing machines. *Physical Review E*, 92(4), October 2015.
 - [27] Artemy Kolchinsky and David H. Wolpert. Thermodynamic costs of turing machines. *Physical Review Research*, 2(3), August 2020.
 - [28] N. Gershenfeld. Signal entropy and the thermodynamics of computation. *IBM Systems Journal*, 35(3.4):577–586, 1996.
 - [29] Takahiro Sagawa. Thermodynamic and logical reversibilities revisited. *Journal of Statistical Mechanics: Theory and Experiment*, 2014(3):P03025, 2014.
 - [30] David H Wolpert and Artemy Kolchinsky. Thermodynamics of computing with circuits. *New Journal of Physics*, 22(6):063047, 2020.
 - [31] David H Wolpert, Artemy Kolchinsky, and Jeremy A Owen. A space–time tradeoff for implementing a function with master equation dynamics. *Nature communications*, 10(1):1–9, 2019.
 - [32] Sosuke Ito and Takahiro Sagawa. Information thermodynamics on causal networks. *Physical review letters*, 111(18):180603, 2013.
 - [33] Sosuke Ito and Takahiro Sagawa. Information flow and entropy production on bayesian networks. *Mathematical Foundations and Applications of Graph Entropy*, 6:63–99, 2016.
 - [34] David H Wolpert. Uncertainty relations and fluctuation theorems for bayes nets. *Physical Review Letters*, 125(20):200602, 2020.
 - [35] Claude E Shannon. The synthesis of two-terminal switching circuits. *The Bell System Technical Journal*, 28(1):59–98, 1949.
 - [36] Udo Seifert. Stochastic thermodynamics: From principles to the cost of precision. *Physica A: Statistical Mechanics and its Applications*, 504:176–191, 2018.
 - [37] Massimiliano Esposito, Katja Lindenberg, and Christian Van den Broeck. Entropy production as correlation between system and reservoir. *New Journal of Physics*, 12(1):013013, 2010.
 - [38] Massimiliano Esposito. Stochastic thermodynamics under coarse graining. *Physical Review E—Statistical, Non-*

- linear, and Soft Matter Physics*, 85(4):041125, 2012.
- [39] David H Wolpert. The free energy requirements of biological organisms; implications for evolution. *Entropy*, 18(4):138, 2016.
- [40] Takahiro Sagawa and Masahito Ueda. Generalized jarzynski equality under nonequilibrium feedback control. *Physical review letters*, 104(9):090602, 2010.
- [41] Takahiro Sagawa and Masahito Ueda. Fluctuation theorem with information exchange: Role of correlations? format? in stochastic thermodynamics. *Physical review letters*, 109(18):180602, 2012.

Appendix A: Derivation of Eq. (25)

1. Subsystem process

Consider a system composed of two subsystems A and B with state space \mathcal{X}_μ and \mathcal{X}_B respectively. A process that evolves initial distribution $p_{AB}^0(x_A, x_B)$ over the joint state space $\mathcal{X}_\mu \times \mathcal{X}_B$ is called a *subsystem process* if the two subsystem evolve independent of each other during the process

$$G_{AB}(x'_A, x'_B | x_A, x_B) = G_A(x'_A | x_A) G_B(x'_B | x_B) \quad (\text{A1})$$

and entropy flow of the joint system is the sum of the entropy flow of the subsystems,

$$Q(p_{AB}^0) = Q_A(p_A^0) + Q_B(p_B^0) \quad (\text{A2})$$

where $Q_A(p_A^0)$ and $Q_B(p_B^0)$ can be referred as *subsystem EF*.

If $q^0(x_A)$ and $q^0(x_B)$ are the prior distributions for the evolution of subsystems A and B respectively, the prior distribution for the joint evolution of A and B , such that condition (A1) and (A2) hold, is the product distribution,

$$q_{AB}^0(x_A, x_B) = q_A^0(x_A) q_B^0(x_B) \quad (\text{A3})$$

2. MMC lower bound on EP of a subsystem process

Consider a system S consisting of multiple subsystems that evolve one after another, and the dynamics of one or more of these subsystems does not directly depend on the state of some other subsystems. In particular, let us focus on a subsystem μ that evolves based on the value of another subsystem denoted as $\text{pa}(\mu)$. The set of the rest of the subsystems is denoted as $\tilde{\mu}$. This results in a particular partition of the set of subsystems, $S = \mu \cup \text{pa}(\mu) \cup \tilde{\mu}$. Let p and \hat{p} denote the probability distribution of the joint system before and after the update of subsystem μ , respectively, while the rest of the system remains unchanged. The distribution undergoes a change,

$$p^\mu(\mathbf{x}_\mu, \mathbf{x}_{\text{pa}(\mu)}, \mathbf{x}_{\tilde{\mu}}) \longrightarrow p^{\mu+1}(\mathbf{x}_\mu, \mathbf{x}_{\text{pa}(\mu)}, \mathbf{x}_{\tilde{\mu}}), \quad (\text{A4})$$

such that $p_{\mu, \text{pa}(\mu)}^{\mu+1}(\mathbf{x}_\mu, \mathbf{x}_{\text{pa}(\mu)}) = \sum_{\mathbf{x}_{\tilde{\mu}}} p^{\mu+1}(\mathbf{x}) = \pi_\mu(\mathbf{x}_\mu | \mathbf{x}_{\text{pa}(\mu)}) p_\mu^\mu(\mathbf{x}_\mu)$, and since the rest of the subsystems do not change, we have $p_{\tilde{\mu}}^{\mu+1}(\mathbf{x}_{\tilde{\mu}}) = \sum_{\mathbf{x}_\mu, \mathbf{x}_{\text{pa}(\mu)}} p^{\mu+1}(\mathbf{x}) = p_{\tilde{\mu}}^\mu(\mathbf{x}_{\tilde{\mu}})$.

As mentioned above in App. A1, the prior distribution for this kind of subsystem process is a product distribution of the form $q^\mu(\mathbf{x}) = q^\mu(\mathbf{x}_\mu, \mathbf{x}_{\text{pa}(\mu)}) q^\mu(\mathbf{x}_{\tilde{\mu}})$. Under the evolution of the subsystem μ conditioned on the state of subsystem $\text{pa}(\mu)$, the prior distribution evolves to $q^{\mu+1}(\mathbf{x}) = q^{\mu+1}(\mathbf{x}_\mu, \mathbf{x}_{\text{pa}(\mu)}) q^\mu(\mathbf{x}_{\tilde{\mu}})$.

$$q^\mu(\mathbf{x}_\mu, \mathbf{x}_{\text{pa}(\mu)}) q^\mu(\mathbf{x}_{\tilde{\mu}}) \longrightarrow q^{\mu+1}(\mathbf{x}_\mu, \mathbf{x}_{\text{pa}(\mu)}) q^\mu(\mathbf{x}_{\tilde{\mu}}) \quad (\text{A5})$$

where $q_{\mu, \text{pa}(\mu)}^{\mu+1}(\mathbf{x}_\mu, \mathbf{x}_{\text{pa}(\mu)}) = \pi_\mu(\mathbf{x}_\mu | \mathbf{x}_{\text{pa}(\mu)}) q_{\text{pa}(\mu)}^\mu(\mathbf{x}_{\text{pa}(\mu)})$.

The mismatch cost of the subsystem process is given by,

$$\mathcal{MC}_\mu = D(p^\mu \| q^\mu) - D(p^{\mu+1} \| q^{\mu+1}) \quad (\text{A6})$$

where the first KL divergence can be written as,

$$D(p^\mu \| q^\mu) = I_\mu(X_\mu, X_{\text{pa}(\mu)}; X_{\tilde{\mu}}) + D(p_{\mu, \text{pa}(\mu)}^\mu \| q_{\mu, \text{pa}(\mu)}^\mu) + D(p_{\tilde{\mu}}^\mu \| q_{\tilde{\mu}}^\mu), \quad (\text{A7})$$

and the second KL divergence,

$$D(p^{\mu+1} \| q^{\mu+1}) = I_{\mu+1}(X_\mu, X_{\text{pa}(\mu)}; X_{\tilde{\mu}}) + D(p_{\mu, \text{pa}(\mu)}^{\mu+1} \| q_{\mu, \text{pa}(\mu)}^{\mu+1}) + D(p_{\tilde{\mu}}^{\mu+1} \| q_{\tilde{\mu}}^{\mu+1}). \quad (\text{A8})$$

Since $p_{\mu, \text{pa}(\mu)}^{\mu+1}(\mathbf{x}_\mu, \mathbf{x}_{\text{pa}(\mu)}) = \pi_\mu(\mathbf{x}_\mu | \mathbf{x}_{\text{pa}(\mu)}) p_{\text{pa}(\mu)}^\mu(\mathbf{x}_{\text{pa}(\mu)})$ and $q_{\mu, \text{pa}(\mu)}^{\mu+1}(\mathbf{x}_\mu, \mathbf{x}_{\text{pa}(\mu)}) = \pi_\mu(\mathbf{x}_\mu | \mathbf{x}_{\text{pa}(\mu)}) q_{\text{pa}(\mu)}^\mu(\mathbf{x}_{\text{pa}(\mu)})$, therefore, using chain rule for KL divergence, $D(p_{\mu, \text{pa}(\mu)}^{\mu+1} \| q_{\mu, \text{pa}(\mu)}^{\mu+1}) = D(p_{\text{pa}(\mu)}^\mu \| q_{\text{pa}(\mu)}^\mu)$. Therefore,

$$D(p^{\mu+1} \| q^{\mu+1}) = I_{\mu+1}(X_\mu, X_{\text{pa}(\mu)}; X_{\tilde{\mu}}) + D(p_{\text{pa}(\mu)}^\mu \| q_{\text{pa}(\mu)}^\mu) + D(p_{\tilde{\mu}}^{\mu+1} \| q_{\tilde{\mu}}^{\mu+1}) \quad (\text{A9})$$

Combining equation (A7) and (A9), the mismatch cost can be written as,

$$\mathcal{MC}_\mu = I_\mu(X_\mu, X_{\text{pa}(\mu)}; X_{\tilde{\mu}}) - I_{\mu+1}(X_\mu, X_{\text{pa}(\mu)}; X_{\tilde{\mu}}) + D(p_{\mu, \text{pa}(\mu)}^\mu \| q_{\mu, \text{pa}(\mu)}^\mu) - D(p_{\text{pa}(\mu)}^\mu \| q_{\text{pa}(\mu)}^\mu) \quad (\text{A10})$$

As an aside, Eq. (A10) provides an alternative derivation of the mutual information contribution to entropy production in systems with multiple communicating components—such as those involved in feedback control protocols—as previously derived in [40, 41] and [34]. Specifically, it emphasizes that the contribution to entropy production arising from the making and breaking of correlations among components in a non-equilibrium process is captured by the MMC.

Note: for simplicity we drop the superscripts (which indicates what step of the computation are we in) and we leave the subscripts (which indicates which gate (or layer) we are updating) since we update sequentially in (A11).

3. Application of subsystem MMC to circuits

When a gate or a layer of gates in a circuit is updated based on the state of the parent gates (or parent layers) while the rest of the circuit remains unchanged, it constitutes a subsystem process. Once again, let us use μ to denote a non-input gate or layer of gates. As described in Sec III A 3, under the update of gate or layer μ , the actual distribution of the circuit changes from $p^\mu(\mathbf{x}) = p_{\cdot, \mu}(\mathbf{x}_{\cdot, \mu}) p_{\mu, \cdot}(\mathbf{x}_\mu, \mathbf{x}_{\cdot})$ to $p^{\mu+1}(\mathbf{x}) = p_{\cdot, \mu, \mu}(\mathbf{x}_{\cdot, \mu}, \mathbf{x}_\mu) p_{\mu, \cdot}(\mathbf{x}_{\cdot})$.

Using Eq. (A10), the mismatch cost of running gate μ is given by the expression,

$$\mathcal{MC}_\mu = I_\mu(X_\mu, X_{\text{pa}(\mu)}; X_{\tilde{\mu}}) - I_{\mu+1}(X_\mu, X_{\text{pa}(\mu)}; X_{\tilde{\mu}}) + D(p_{\mu, \text{pa}(\mu)} \| q_{\mu, \text{pa}(\mu)}) - D(p_{\text{pa}(\mu)} \| q_{\text{pa}(\mu)}) \quad (\text{A11})$$

where $I_\mu(X_\mu, X_{\text{pa}(\mu)}; X_{\tilde{\mu}})$ and $I_{\mu+1}(X_\mu, X_{\text{pa}(\mu)}; X_{\tilde{\mu}})$ are the mutual information between $(\mu, \text{pa}(\mu))$ and the rest of the circuit before and after updating gate μ , respectively. Denote by ΔI_μ the change in mutual information due to the update of gate μ ,

$$\Delta I_\mu = I_\mu(X_\mu, X_{\text{pa}(\mu)}; X_{\tilde{\mu}}) - I_{\mu+1}(X_\mu, X_{\text{pa}(\mu)}; X_{\tilde{\mu}}). \quad (\text{A12})$$

Considering $I_\mu(X_\mu, X_{\text{pa}(\mu)}; X_{\tilde{\mu}})$, i.e., the mutual information between $(\mu, \text{pa}(\mu))$ and $\tilde{\mu}$ before the gate μ is updated:

$$I_\mu(X_\mu, X_{\text{pa}(\mu)}; X_{\tilde{\mu}}) = S_\mu(X_\mu, X_{\text{pa}(\mu)}) + S_\mu(X_{\tilde{\mu}}) - S_\mu(X_\mu, X_{\text{pa}(\mu)}, X_{\tilde{\mu}}) \quad (\text{A13})$$

$$= S_\mu(X_\mu) + S_\mu(X_{\text{pa}(\mu)}) + S_\mu(X_{\tilde{\mu}}) - S_\mu(X), \quad (\text{A14})$$

where in the second equality we have used the independence of μ and $\text{pa}(\mu)$ before μ is updated and $S_\mu(X) = S_\mu(X_\mu, X_{\text{pa}(\mu)}, X_{\tilde{\mu}})$ is used to denote the entropy of the joint system before gate μ is updated. Now, consider the mutual information after gate μ is updated:

$$I_{\mu+1}(X_\mu, X_{\text{pa}(\mu)}; X_{\tilde{\mu}}) = S_{\mu+1}(X_\mu, X_{\text{pa}(\mu)}) + S_{\mu+1}(X_{\tilde{\mu}}) - S_{\mu+1}(X). \quad (\text{A15})$$

Note that $S_{\mu+1}(X_{\tilde{\mu}}) = S_{\mu}(X_{\tilde{\mu}})$ because the marginal distribution over the rest of the circuit $\tilde{\mu}$ does not change as μ is updated. Moreover, $S_{\mu}(X_{\mu}) + S_{\mu}(X_{\text{pa}(\mu)}) - S_{\mu+1}(X_{\mu}, X_{\text{pa}(\mu)}) = I_{\mu+1}(X_{\mu}; X_{\text{pa}(\mu)})$, i.e., the mutual information between μ and $\text{pa}(\mu)$ after μ is updated. Therefore, the change in mutual information obtained by subtracting (A13) from (A15) is

$$\Delta I_{\mu} = I_{\mu} - I_{\mu+1} \quad (\text{A16})$$

$$= I_{\mu+1}(X_{\mu}; X_{\text{pa}(\mu)}) + S_{\mu+1}(X) - S_{\mu}(X). \quad (\text{A17})$$

When ΔI_{μ} contributions are summed over all the non-input gates in the circuit (in any topological order), we get:

$$\sum_{\mu \in V} \Delta I_{\mu} = \sum_{\mu \in V_{\text{nin}}} [I_{\mu+1}(X_{\mu}; X_{\text{pa}(\mu)}) + S_{\mu+1}(X) - S_{\mu}(X)] \quad (\text{A18})$$

$$= S_{|V_{\text{nin}}|+1}(X) - S_1(X) + \sum_{\mu \in V_{\text{nin}}} I_{\mu+1}(X_{\mu}; X_{\text{pa}(\mu)}) \quad (\text{A19})$$

Eq. (A19) is consistent with earlier results on the loss of mutual information in Bayesian networks considered in [34]. [34] considers thermodynamic analysis of more general Bayesian networks with branches, loops, recurrence, etc. Note that $S_1(X)$ denote the Shannon entropy of the joint circuit state before any non-input gates are run on the new inputs, and $S_{|V_{\text{nin}}|+1}(X)$ is the entropy after all non-input gates have completed their updates.

Before any non-input gates are executed, the values stored in the non-input nodes X_{nin} are remnants of the previous run, while the input nodes X_{in} are freshly sampled from the new input distribution. By construction of the model, these two collections of variables are initially statistically independent. Therefore,

$$S_1(X) = S_1(X_{\text{nin}}, X_{\text{in}}) = S_1(X_{\text{nin}}) + S_1(X_{\text{in}}). \quad (\text{A20})$$

After the circuit has finished updating, the non-input nodes generally become correlated with the inputs through the computation. Hence, the final joint entropy can be written as

$$S_{|V_{\text{nin}}|+1}(X) = S(X_{\text{nin}}, X_{\text{in}}), \quad (\text{A21})$$

Combining these expressions, we obtain

$$S_1(X) - S_{|V_{\text{nin}}|+1}(X) = S_1(X_{\text{nin}}) + S_1(X_{\text{in}}) - S(X_{\text{nin}}, X_{\text{in}}) = I_0(X_{\text{nin}}; X_{\text{in}}). \quad (\text{A22})$$

where $I_0(X_{\text{nin}}; X_{\text{in}})$ denotes the mutual information between the non-input and input nodes induced by the computation, before inputs are provided with new values and the entire circuit is correlated from the previous run. Therefore, the aggregate mismatch cost of running all non-input gates sequential is

$$\sum_{\mu} \mathcal{MC}_{\mu} = -I_0(X_{\text{nin}}; X_{\text{in}}) + \sum_{\mu \in V_{\text{nin}}} I_{\mu+1}(X_{\mu}; X_{\text{pa}(\mu)}) + \sum_{\mu \in V_{\text{nin}}} [D(p_{\mu} p_{\text{pa}(\mu)} || q_{\mu, \text{pa}(\mu)}) - D(p_{\text{pa}(\mu)} || q_{\text{pa}(\mu)})] \quad (\text{A23})$$

This mismatch cost of overwriting the input nodes with new values sampled from p_{in} is given by Eq. 19:

$$\mathcal{MC}_{ow}(p_{\text{in}}) = I_0(X_{\text{in}}; X_{\text{nin}}) + D(p_{\text{in}} || q_{\text{in}}). \quad (\text{A24})$$

Total mismatch cost of the circuit is the sum of mismatch cost of overwriting the input nodes with new values and the aggregate mismatch cost of running all non-input gates. Thus, for an input distribution p_{in} and circuit C_n , the total mismatch cost is

$$\mathcal{MC}(C_n, p_{\text{in}}) = \mathcal{MC}_{ow}(p_{\text{in}}) + \sum_{\mu \in V_{\text{nin}}} \mathcal{MC}_{\mu} \quad (\text{A25})$$

$$= D(p_{\text{in}} || q_{\text{in}}) + \sum_{\mu \in V_{\text{nin}}} I_{\mu+1}(X_{\mu}; X_{\text{pa}(\mu)}) + \sum_{\mu \in V_{\text{nin}}} [D(p_{\mu} p_{\text{pa}(\mu)} || q_{\mu, \text{pa}(\mu)}) - D(p_{\text{pa}(\mu)} || q_{\text{pa}(\mu)})]. \quad (\text{A26})$$

Appendix B: Proofs

1. Proof of Thm. 1

From Eq. (A26), we have:

$$\mathcal{MC}(C_n, p_{\text{in}}) = D(p_{\text{in}} \| q_{\text{in}}) + \sum_{\mu \in V_{\text{nin}}} (\mathbb{I}_{\mu+1}(X_\mu; X_{\text{pa}(\mu)}) + \Delta_\mu), \quad (\text{B1})$$

where

$$\Delta_\mu := D(p_\mu p_{\text{pa}(\mu)} \| q_{\mu, \text{pa}(\mu)}) - D(p_{\text{pa}(\mu)} \| q_{\text{pa}(\mu)}). \quad (\text{B2})$$

We assume that the prior distribution $q_{\mu, \text{pa}(\mu)}$ is a product distribution, i.e.,

$$q_{\mu, \text{pa}(\mu)}(\mathbf{x}_\mu, \mathbf{x}_{\text{pa}(\mu)}) = q_\mu(\mathbf{x}_\mu) q_{\text{pa}(\mu)}(\mathbf{x}_{\text{pa}(\mu)}), \quad (\text{B3})$$

for every joint state $(\mathbf{x}_\mu, \mathbf{x}_{\text{pa}(\mu)})$. Then, Δ_μ simplifies as follows:

$$\Delta_\mu = D(p_\mu p_{\text{pa}(\mu)} \| q_\mu q_{\text{pa}(\mu)}) - D(p_{\text{pa}(\mu)} \| q_{\text{pa}(\mu)}) \quad (\text{B4})$$

$$= D(p_\mu \| q_\mu) + D(p_{\text{pa}(\mu)} \| q_{\text{pa}(\mu)}) - D(p_{\text{pa}(\mu)} \| q_{\text{pa}(\mu)}) \quad (\text{B5})$$

$$= D(p_\mu \| q_\mu) \quad (\text{B6})$$

We also have

$$\mathbb{I}_{\mu+1}(X_\mu; X_{\text{pa}(\mu)}) = S(X_\mu) - S_{\mu+1}(X_\mu | X_{\text{pa}(\mu)}), \quad (\text{B7})$$

where $S(X_\mu) = -\sum_{\mathbf{x}_\mu} p_\mu(\mathbf{x}_\mu) \log p_\mu(\mathbf{x}_\mu)$, and $S_{\mu+1}(X_\mu | X_{\text{pa}(\mu)})$ is the conditional entropy of the state of gate μ given the states of its parents $\text{pa}(\mu)$ after the gate has been run. For deterministic gates, $S_{\mu+1}(X_\mu | X_{\text{pa}(\mu)}) = 0$. More generally, since conditional entropy is non-negative, we have the bound

$$\mathbb{I}_{\mu+1}(X_\mu; X_{\text{pa}(\mu)}) \leq S(X_\mu). \quad (\text{B8})$$

Moreover, the KL divergence can be written as

$$D(p_\mu \| q_\mu) = \mathcal{C}(p_\mu \| q_\mu) - S(X_\mu), \quad (\text{B9})$$

where $\mathcal{C}(p_\mu \| q_\mu)$ denotes the cross-entropy of p_μ relative to q_μ .

Combining Eqs. (B8) and (B9), we obtain the upper bound

$$\sum_{\mu \in V_{\text{nin}}} (\mathbb{I}_{\mu+1}(X_\mu; X_{\text{pa}(\mu)}) + \Delta_\mu) \leq \sum_{\mu \in V_{\text{nin}}} \mathcal{C}(p_\mu \| q_\mu). \quad (\text{B10})$$

Furthermore, for any distribution p_μ , the cross-entropy satisfies

$$\mathcal{C}(p_\mu \| q_\mu) \leq \log \left(\frac{1}{q_\mu^{\min}} \right), \quad (\text{B11})$$

where

$$q_\mu^{\min} := \min_x q_\mu(x). \quad (\text{B12})$$

If all gates share the same prior, i.e., $q_\mu = q_g$ for all μ (subscript g implies non-input gate), this yields

$$\sum_{\mu \in V_{\text{nin}}} (\mathbb{I}_{\mu+1}(X_\mu; X_{\text{pa}(\mu)}) + \Delta_\mu) \leq |C_n| \log \left(\frac{1}{q_g^{\min}} \right), \quad (\text{B13})$$

where $|C_n|$ denotes the number of gates in the circuit.

To obtain an explicit upper bound on the KL divergence $D(p_{\text{in}}||q_{\text{in}})$ in terms of the input length n , we assume that the prior distribution over the joint state of the input nodes factorizes across input bits:

$$q_{\text{in}}(\mathbf{x}_{\text{in}}) = q_{\text{in}}(x_{\text{in},1}, \dots, x_{\text{in},n}) = \prod_{k=1}^n q_{\text{in},k}(x_{\text{in},k}). \quad (\text{B14})$$

Moreover, we assume that all marginals are identical, i.e., $q_{\text{in},k} = q_i$ for all k (subscript i implies input nodes). Then, using sub-additivity of KL divergence under product priors, we have

$$D(p_{\text{in}}||q_{\text{in}}) \leq \sum_{k=1}^n D(p_k||q_i), \quad (\text{B15})$$

where p_k denotes the marginal of p_{in} on the k -th input node. Since each term is bounded by

$$D(p_k||q_i) \leq \log\left(\frac{1}{q^{\min}}\right), \quad (\text{B16})$$

with $q_i^{\min} := \min_x q_i(x)$, it follows that

$$D(p_{\text{in}}||q_{\text{in}}) \leq n \log\left(\frac{1}{q_i^{\min}}\right) = nK_{\text{in}}, \quad (\text{B17})$$

where $K_{\text{in}} := \log\left(\frac{1}{q_i^{\min}}\right)$. This bound is worst-case over all input distributions p_{in} and depends only on the minimal support of the prior q .

Combining Eq. (B13) and (B17), and substituting them in (B1), we obtain the worst-case upper bound over all input distributions p_{in} on the total mismatch cost of a circuit:

$$\mathcal{MC}(C_n) \leq |C_n|K + nK_{\text{in}}. \quad (\text{B18})$$

where $K = \log\left(\frac{1}{q_g^{\min}}\right)$ and $K_{\text{in}} = \log\left(\frac{1}{q_{\text{in}}^{\min}}\right)$.

2. Proof of Thm. 2

To derive the bound (B18), we assumed that all the gates in the circuit have the same prior distribution. But this assumption can be dropped by allowing different logic gates to have different priors. Let \mathcal{B} be a basis of logic gates, and let q_g denote the prior distribution associated with each gate type $g \in \mathcal{B}$. Let $\#_g(n)$ be the number of gates of type g appearing in a circuit C_n of size n . (Here, the size of C_n counts only non-input logic gates.) Define

$$K_g := \log\left(\frac{1}{q_g^{\min}}\right), \quad (\text{B19})$$

where $q_g^{\min} := \min_x q_g(x)$.

By Eqs. (B8), (B9), and (B11), each term in the sum on the right-hand side of Eq. (B1) is upper bounded. In particular, if gate μ is of type g , then

$$I_{\mu+1}(X_\mu; X_{\text{pa}(\mu)}) + \Delta_\mu \leq K_g. \quad (\text{B20})$$

Therefore, if there are $\#_g(n)$ gates of type g in the circuit, we obtain

$$\sum_{\mu \in V_{\text{in}}} (I_{\mu+1}(X_\mu; X_{\text{pa}(\mu)}) + \Delta_\mu) \leq \sum_{g \in \mathcal{B}} \#_g(n)K_g. \quad (\text{B21})$$

The total mismatch cost is bounded by

$$\mathcal{MC}(C_n, p_{\text{in}}) \leq \sum_{g \in \mathcal{B}} \#_g(n)K_g + nK_{\text{in}}. \quad (\text{B22})$$

We can equivalently write the summation term as

$$\sum_{g \in \mathcal{B}} \#_g(n), K_g = |C_n| \sum_{g \in \mathcal{B}} \gamma_g(n) K_g, \quad (\text{B23})$$

where $\gamma_g(n) := \#_g(n)/|C_n|$ is the fraction of gates of type g in C_n .

If $\gamma_g(n)$ converges to a constant γ_g as n grows large (or if γ_g is a constant for all n), then we recover an upper bound analogous to Theorem (1):

$$\mathcal{MC}(C_n) \leq |C_n| K' + n K_{\text{in}}, \quad (\text{B24})$$

where

$$K' := \sum_{g \in \mathcal{B}} \gamma_g, K_g. \quad (\text{B25})$$

3. Circuit as a periodic process

A circuit can be viewed as a periodic process when a counter is integrated into its description. The counter can differentiate one clock cycle from another and sequentially run different layers or gates with each clock cycle. The periodic process, governed by the clock cycle, repeats over and over again, but sequentially implements different gates or layers with each clock cycle.

Let Z denote the random variable representing the state of the counter, taking values $z \in \{0, 1, \dots\}$. The joint state of the system is given by (\mathbf{x}, z) , where \mathbf{x} is the state of the circuit and z is the state of the counter. We let μ index the sequence of gates or layers in the circuit. Let $p_{X,Z}(\mathbf{x}, z)$ denote the probability distribution over the joint state, which can be expressed as a conditional distribution of \mathbf{x} given the state of the counter:

$$p_{X,Z}(\mathbf{x}, z) = p_{X|Z}(\mathbf{x}|z) p_Z(z) \quad (\text{B26})$$

At the beginning of a circuit run, the counter is initialized to $\mu = 0$. With each gate execution, the counter increments by one. Therefore, prior to the execution of gate μ , the counter is in state $z = \mu$. The distribution over circuit states just before the execution of gate μ is then given by

$$p_{X,Z=\mu}(\mathbf{x}) = p_{X|Z=\mu}(\mathbf{x}), \quad (\text{B27})$$

indicating that the counter is precisely in state μ . Note that $p_{X|Z=\mu}(\mathbf{x})$ corresponds to $p^\mu(\mathbf{x})$, consistent with the notation used throughout the paper and as summarized in Table (I).

The prior distribution $q_{X,Z}$ represents the full full process that is repeated with each clock cycle of the circuit. Accordingly, the prior over the joint state (\mathbf{x}, z) can be expressed as

$$q_{X,Z}(\mathbf{x}, z) = q_{X|Z}(\mathbf{x} | z), q_Z(z), \quad (\text{B28})$$

and evolves under the periodic dynamics of the circuit to

$$\tilde{q}_{X,Z}(\mathbf{x}, z) = \tilde{q}_{X|Z}(\mathbf{x} | z), \tilde{q}_Z(z), \quad (\text{B29})$$

where $\tilde{q}_{X|Z}$ denotes the updated distribution over circuit states following one cycle of evolution.

The prior distribution q^μ , associated with the execution of gate μ , is now understood as being conditioned on the counter state. In particular, the prior distribution over circuit states just before the execution of gate μ (i.e., when the counter is in state $z = \mu$) is given by

$$q_{X,Z=\mu}(\mathbf{x}) = q_{X|Z}(\mathbf{x} | z), q_{Z=\mu}(z), \quad (\text{B30})$$

where $q_{Z=\mu}(z) = \delta_{z,\mu}$ is a delta distribution, enforcing that the counter is precisely in state μ . Equivalently, this can be written more concisely as

$$q_{X,Z=\mu}(\mathbf{x}) = q_{X|Z=\mu}(\mathbf{x}). \quad (\text{B31})$$

Applying the MMC formula to the execution of gate μ , we obtain

$$\mathcal{MC}_\mu = D(p_{X|Z=\mu} \| q_{X|Z=\mu}) - D(p_{X|Z=\mu+1} \| \tilde{q}_{X|Z=\mu}), \quad (\text{B32})$$

which, under the earlier notation $p^\mu = p_{X|Z=\mu}$, $q^\mu = q_{X|Z=\mu}$, and $\tilde{q}^\mu = \tilde{q}_{X|Z=\mu}$, becomes

$$\mathcal{MC}_\mu = D(p^\mu \| q^\mu) - D(p^{\mu+1} \| \tilde{q}^\mu), \quad (\text{B33})$$

which coincides with Eq. (22).

4. Further analysis of mutual information terms

Another way to factor out eq (A12)

$$\Delta I_\mu = I_\mu(X_\mu, X_{\text{pa}(\mu)}; X_{\bar{\mu}}) - I_{\mu+1}(X_\mu, X_{\text{pa}(\mu)}; X_{\bar{\mu}}). \quad (\text{B34})$$

By applying the chain rule for mutual information we get:

$$\begin{aligned} \Delta I_\mu &= \left[I_\mu(X_{\text{pa}(\mu)}; X_{\bar{\mu}}) + I_\mu(X_\mu; X_{\bar{\mu}} | X_{\text{pa}(\mu)}) \right] \\ &\quad - \left[I_{\mu+1}(X_{\text{pa}(\mu)}; X_{\bar{\mu}}) + I_{\mu+1}(X_\mu; X_{\bar{\mu}} | X_{\text{pa}(\mu)}) \right]. \end{aligned}$$

Since the parents $X_{\text{pa}(\mu)}$ do not change between μ and $\mu + 1$, the first two terms cancel:

$$\Delta I_\mu = I_\mu(X_\mu; X_{\bar{\mu}} | X_{\text{pa}(\mu)}) - I_{\mu+1}(X_\mu; X_{\bar{\mu}} | X_{\text{pa}(\mu)}). \quad (\text{B35})$$

For a deterministic gate, after the update $X_{\mu+1} = f(X_{\text{pa}(\mu)})$, the gate output is completely determined by its parents, implying $X_{\mu+1} \perp\!\!\!\perp X_{\bar{\mu}} | X_{\text{pa}(\mu)}$, and therefore

$$I_{\mu+1}(X_\mu; X_{\bar{\mu}} | X_{\text{pa}(\mu)}) = 0, \quad \Rightarrow \quad \Delta I_\mu = I_\mu(X_\mu; X_{\bar{\mu}} | X_{\text{pa}(\mu)}). \quad (\text{B36})$$

Now decompose $X_{\bar{\mu}}$ into the circuit's *past* and *future* relative to the update order:

$$X_{\bar{\mu}} = (X_{:\mu}, X_{\mu:}).$$

In a feed-forward (topologically ordered) circuit, $X_{:\mu}$ contains no additional information about X_μ once $X_{\text{pa}(\mu)}$ is given: $I_\mu(X_\mu; X_{:\mu} | X_{\text{pa}(\mu)}) = 0$. Hence,

$$\begin{aligned} \Delta I_\mu &= I_\mu(X_\mu; X_{:\mu}, X_{\mu:} | X_{\text{pa}(\mu)}) \\ &= I_\mu(X_\mu; X_{:\mu} | X_{\text{pa}(\mu)}) + I_\mu(X_\mu; X_{\mu:} | X_{\text{pa}(\mu)}, X_{:\mu}) \\ &= I_\mu(X_\mu; X_{\mu:} | X_{\text{pa}(\mu)}). \end{aligned} \quad (\text{B37})$$

(When appropriate—for deterministic, acyclic circuits with fixed parents—the conditioning can be dropped, giving $I_\mu(X_\mu; X_{\mu:})$)